Norwegian University of Life Sciences

Master's Thesis 2021 60 ECTS

Department of Animal and Aquaculture Sciences Norwegian University of Life Sciences

A STUDY OF TWO ADIPOSE TISSUE DEPOTS IN ATLANTIC SALMON

Yi Yuan

Aquaculture

A STUDY OF TWO ADIPOSE TISSUE DEPOTS IN ATLANTIC SALMON

With specific focus on comparing the morphological and transcriptome characteristics between visceral and subcutaneous adipocytes

Master thesis (60 credits)

Yi Yuan

Department of Animal and Aquaculture Sciences
Norwegian University of Life Sciences

Ås
2021

Acknowledgement

Funding for the experiment was from the project named. The practical work presented in this thesis was carried out at Nofima Marin. All the support is gratefully acknowledged.

This thesis was accomplished under the supervision of Bente Ruyter, Marta Bou Mira, and Esmail Lutfi Royo. I hereby express my sincere gratefulness to all my supervisors for appreciating their careful guidance in the field of fish nutrition, lab work, and academics English. I believe what I learned from them not only benefits my school career but also my future life. Thanks again for all your caring and patience throughout this period, encouraging me with a hard-working and serious attitude toward science. Besides, I sincerely appreciated the chance provided by my supervisor Bente, which I could visit my family during COVID-19 was getting prevalent. To Marta and Esmail, I do enjoy working with you guys and thank you for creating an energetic and relaxing atmosphere at the lab, which helps me a lot to quickly integrate myself with the new working environment.

Lots of love and thanks to my parents and the other family members. Without your support and encouragement, I did not believe studying abroad can be possible. Even though I rarely visit the home during these two years, your caring through the phone made me know that you always are the people behind me, supporting and understanding me.

Thanks to my girlfriend Sissi for the company during thesis writing. You always support me and bring a good mood with me when I'm frustrating, which made me believe writing work was not difficult. And to my friends, Puchun, Ke, and those who I have not named. As you guys said 'working hard, play hard', I have spent good and happy times after school, which made me energetic back to work.

Special thanks to my advisor Stine Telneset for your suggestions and instructions to my student career, which made it much easier for me to overcome those difficulties and frustrating periods in my study life.

Ås, Oct. 2020
Yi Yuan

Table of content

Contents

Abbreviations

ADP	Adenosine diphosphate
AT	Adipose tissue
ATP	Adenosine triphosphate
A1M	Alpha-1-microglobulin
aSVF	Adipose-drived stromal-vascular fraction
cAMP	Cyclic adenosine monophosphate
CEL	Carboxyl ester lipase
CK	Creatine kinase
CP	Carboxypeptidases
CPT	Carnitine palmitoyl-transferase
DAPI	4’,6-diamidino-2-phentlindole
DHAP	Dihydroxyacetone phosphate
DEX	Dexamethasone
DPEP1	Dipeptidase 1
ECM	Extracellular matrix
ELA1	Elastase-1
FA(s)	Fatty acid(s)
FBS	Fetal bovine serum
FFAs	Free fatty acids
F6P	Fructose-6-phosphate
GM	Growth media
GM-CSF	Granulocyte-macrophage colony stimulating factor
GPBB	Glycogen phosphorylase brain
GPDH	Glycerol-3-phosphate dehydrogenase
GPI	Glucose-6-phosphate isomerase
G1P	Glucose 1-phosphate
G3P	Glyceraldehyde-3-phosphate
G6P	Glucose-6-phosphate
ITAM	Immunoreceptor tyrosine-based activation motif
IBMX	3-isobutyl-1-methylxantine
IGFs	Insulin-like growth factors
ILs	Interleukins
IFN-γ	Interferon gamma

L-15	Leibowitz-15
LCFA	Long chain fatty acid
MHC	Histocompatibility complex
MPO	Myeloperoxidase
MSCs	Mesenchymal stem cells
NADH	Reduced nicotinamide adenine dinucleotide
PBS	Phosphate buffered saline
PEP	Phosphoenolpyruvate
PFA	Paraformaldehyde
PGK	Phosphoglycerate kinase
PGM1	Phosphoglucomutase 1
PKM2	Pyruvate kinase, muscle
SPARC	Secreted protein acidic and rich in cysteine
TCR	T-cell receptor
TNF	Tumor necrosis factor
TNFR	Tumor necrosis factor receptor
TGF β	Transforming growth factor beta
T3	Triiodothyronine
α	Alpha
β	Beta
γ	Gamma
δ	Delta

Summary

Adipocytes are found in different adipose tissue depots, mainly around abdominal organs (visceral adipose tissue), or under the skin (subcutaneous adipose tissue) and between muscle fibers in myosepta including belly flap. However, the morphological and functional differences between visceral and subcutaneous depots in Atlantic salmon is poorly understood. The main aim of this thesis was therefore to provide novel insights into the functional differences between the depots by studying differences in their gene expressions and morphologies.

In order to study morphological characteristic of adipose depots, microscopy images of slides from three tissue sections (visceral fat tissue, belly flap, and dorsal fat) were taken and then processed by the software ImageJ. The result showed that visceral adipose tissue contained much fewer and larger adipocytes than the two subcutaneous adipose depots from belly flap and dorsal fat. The adipocyte cell size distribution was also analyzed, showing that the belly flap- and the dorsal fat depots contained nearly the same number of adipocytes per area. The data was divided the adipocytes into four cell size ranges: 50-300μm^2, 300-2500μm^2, 2500-7000μm^2, and larger than 7000μm^2. The data indicated that adipocytes within the size range 2500-7000μm^2 had the highest proportion in visceral adipose tissue, while adipocytes within the size range 300-2500μm^2 had the highest proportion in subcutaneous adipose tissue. Moreover, in visceral adipose tissue, there were more extremely big cells compared with in subcutaneous adipose tissue, which had the largest proportion of the smallest adipocytes (50-300μm^2 group).

Since the two subcutaneous fat depots, belly flap and dorsal fat, were quite similar in morphological characterization, only dorsal fat was chosen as representative for subcutaneous adipose tissue for the microarray analyses of gene expression together visceral adipose. Further, pre-adipocytes were isolated from both visceral adipose tissue and dorsal adipose tissue, in order to compare their capacities to proliferate and differentiate to mature adipocytes *in vitro*. After being isolated, visceral and subcutaneous pre-adipocytes were cultivated for 15 days until they mature to differentiated adipocytes. The lipid droplets in cytoplasm of mature adipocytes were stained with Lipid Tox fluorescent Green Stain, and the lipid droplets signal was captured by microscope. We observed that, according to the green signal, many small lipid droplets were widely distributed inside the subcutaneous adipocytes, and only a few lipid droplets were fused into larger ones. In contrast, the bigger and brighter green signal dots were shown in visceral adipocytes, which indicated that there were more, and larger lipid droplets accumulated inside cells. The result demonstrated the capability of individual visceral adipocyte cells to produce more large lipids droplets under the same *in vitro* conditions compared with subcutaneous cells. The vitrification of the

intracellular lipid content level of two types of adipocytes was completed by quantification experiments. Firstly, with Oil red O staining intracellular lipid droplets and Coomassie blue staining protein, lipid droplets and cell nucleus respectively showed bright orange and blue color. Meanwhile, images taken from these two staining methods, both showed that the size of visceral adipocytes was bigger than that of subcutaneous adipocytes, which was also verified with the results from *in vivo* histological analysis. Afterward, by using the spectrometer method to detect the concentration of lipids and protein at 500nm and 630nm, the results versified that *in vitro* differentiated adipocytes from visceral fat visceral fat had stronger abilities to accumulate more lipid droplets than subcutaneous adipocytes.

In conclusion, *in vitro* results showed that visceral adipose tissue contains fewer adipocytes than subcutaneous adipose tissue. But those spherical-shaped visceral adipocytes are in average larger than those fibroblastic-shaped subcutaneous adipocytes. Both *in vivo* and *in vitro* differentiated adipocytes showed that cells from VAT and are capable of accumulating large intracellular lipid droplets than SATs. These two adipose tissue depots showed major differences in expression of genes related to insulin resistance, immunity, energy and lipid metabolism, and extracellular matrix.

The result from the microarray study indicates that VAT possesses insulin resistance, while SAT is prone to insulin sensitivity. The characteristic of VAT with insulin resistance is associated with a higher expression of acute phase proteins and T cells and the higher amount of FFAs, which have been both shown to interfere with insulin activity. In contrast, SAT with insulin-sensitive property is in accordance with higher levels of adiponectin and insulin growth regulating factors, which are accompanied by increases insulin activity.

For those immunity-related genes, they were found mainly related to innate immune and the adaptive system. With the aspect with the innate immune system, higher expression of genes that are involved in the complement system and produce the immune effector molecules are upregulated in VAT compared with SAT. A similar result was found in the adaptive immune system, in which VAT mainly participates the activation and regulation of T cells. However, the expression levels of the genes that belong to the adaptive immune system were not as strong as that of the genes that are implicated in the innate immune system. These results suggest that VAT is more actively participated in the immunity activity in comparison to SAT, serving as a primary coordinator of the innate immune response.

For the energy metabolism in adipose tissue, we observed that the upregulated expression of some metabolic enzyme genes in VAT, indicating the role of SAT that function as a direct free energy supply site compared with VAT that participates in the transportation of FFAs to other organs for β-oxidation.
For lipid metabolism, SAT has been dementated to be more antilipolytic with the elevated expression of some transport proteins indicating the high intracellular Ca2+ concentration in SAT. However, VAT is more metabolically active to lipolysis that is consistent with the transcriptome characteristic of adipose tissue that VAT has the stronger ability to mobilize FFA and less to the anti-lipolytic action of insulin in comparison to SAT.

The genes related to ECM collagen and ECM protein were higher expressed in SAT than VAT. These genes play an essential role in maintaining the function and integrity of ECM. The higher expression of these genes in SAT than VAT demonstrates that, in comparison to VAT, the normal function and integrity of ECM are more necessary to keep the metabolic function of SAT.

In general, VAT not only serves as lipids storage but also participates in the immunity system as a primary coordinator of the innate immune response. SAT mainly functions as a direct energy provider compared with SAT transporting FFAs to other organs. VAT has a strong capability to lipolysis that is closely related to the stronger ability to mobilize FFA and less to the anti-lipolytic action of insulin in comparison to SAT, while SAT has been shown to inhibit lipolytic activity.

1 Introduction

Global interest in white adipose tissue (AT), commonly known as fat tissue, has increased in recent decades because of the increasing prevalence of obesity in both adults and children (Nath et al., 2006). In fish species, a high level of lipids is currently used in the commercial diet to spare the expensive protein consume for muscle growth, resulting in a higher carcass lipids level (Refstie et al., 2001) as well as larger abdominal and myoseptal fat deposits (Bjerkeng et al., 1997). This increased level of fat deposition can result in production loss during processing (Rørå et al., 1998) or even significantly physiological alterations such as the induction of oxidative stress (Kjær et al., 2008). For the prevention of excessive lipid storage in fish, improved knowledge of the development and functions process of preadipocyte to adipocyte and the mechanism underlying the process may provide insight into it. One of the aims of this thesis was from morphology and functional aspects to compare the differences between visceral and subcutaneous adipose tissues.

Adipose tissue is a specialized connective tissue consisting of lipid-rich cells called adipocytes and differs in their locations and morphology characteristic. In fish species, adipose tissue functions as the major fat deposition and the main fat storage sites in fish are mesenteric fat, muscle, and liver(Sheridan, 1988). It was reported that, in Atlantic salmon, the primary sites of fat storage were visceral adipose tissue(Jezierska et al., 1982; Morgan et al., 2002; Rowe et al., 1991) and myosepta, a connective tissue that separates the muscle sheets, allowing for a continuous muscle structure (Zhol et al., 1995; Zhou et al., 1996). This study also showed that adipocytes from Atlantic salmon are mainly distributed in visceral adipose tissue, subcutaneous fat layer, belly flap, and myosepta (Zhou et al., 1996). The distribution of different fat tissues and the size of adipocytes varying between different fish species had also been studied in (carp(Fauconneau et al., 1995); salmon(Zhou et al., 1996); trout(Albalat et al., 2005; Fauconneau et al., 1997); gilthead sea bream(Bou et al., 2014)). However, we hardly found the research presenting the detailed results of the cellular characteristics of different adipose tissues in Atlantic salmon.

On the other hand, as one valuable research method of studying the function of adipocytes, the experiments of cultivating the preadipocytes isolated from visceral adipose tissue to mature adipocytes have been established in Atlantic salmon (Todorčević et al., 2010; Vegusdal et al., 2003). There is also some research showing that human subcutaneous pre-adipocytes can be cultivated (Harms et al., 2019).

Besides, white adipose tissue is now regarded as an important secretory/endocrine organ that produces numerous secretory proteins including adipokines and a suite of small signaling proteins(Gregoire, 2001; Kershaw & Flier, 2004). By the secretion of hormones and cytokines, adipocytes can also function in the regulation of energy metabolism and in immunity in Atlantic salmon (Hutley et al., 2003; Todorčević et al., 2010). But is there any difference between adipose tissue located in different positions when they function as secretory/endocrine organ?

In Atlantic salmon, the preadipocytes from adipose tissue show strong plasticity. *In vitro* experimental, the preadipocytes from visceral fat in Atlantic salmon still showed the potential ability to differentiate to the osteogenic cell lineage (Ytteborg et al., 2015). Since the differentiation process was triggered by the different extracellular matrix (ECM), preadipocytes from adipose tissues were final able to mature to visceral adipocytes or osteogenic cells within the different culture conditions. Besides, the gene transcriptome profile during differentiation showed the difference. This report suggests the potential plasticity existing in the preadipocytes and that the transcriptome expressed differently in the formation of different cell linage.

The final aim of this thesis was, by using the microarray method, to study the expression differences between visceral and subcutaneous adipose tissue, which may provide the new knowledge about the potentially functional difference between those two fat depots.

An aim of this thesis was to study the final differentiated stage of adipocytes by the capacity to store lipids. During the cultivation, the cellular morphology of different adipocytes was also studied and the result from *in vivo* experiments can also be verified. Adipose tissues in Atlantic salmon play a significant role in lipids storage. However, the differences between visceral and subcutaneous adipose tissue relating to lipids accumulating were not clear. Visceral adipose tissue is regarded as the main fat deposition, which may imply that visceral adipocytes were capable of the stronger ability to accumulate lipid droplets. To quantify the intracellular lipids content in different adipocytes, the differentiated visceral and subcutaneous adipocytes were also investigated by immunohistochemistry study.

A major aim of this thesis was to, by histology and gene expression analyses, get new knowledge on different depots (from visceral and dorsal fat tissues and belly flap) size distribution and their function, which may increase the knowledge of the mechanisms involved in the development of fat tissues (hyperplasia/hypertrophy) and further their role in insulin resistance, immunity, energy and lipid metabolism, and extracellular matrix.

2 Literature review

2.1 Adipose tissue characteristics

Adipose tissue is a specialized connective tissue consisting of lipid-rich cells called adipocytes. Connective tissue is one of four basic types of animal tissue, along with epithelial tissue, muscle tissue, and nervous tissue. As one of main connective tissues, adipose tissue develops in certain areas of body, such as visceral fat (around the internal organ), subcutaneous layer (between skin and muscle), in bone marrow (yellow bone marrow), intermuscular (Muscular system) and in the breast (breast tissue). The distribution and the amount of adipose tissue varies differently depending on the species. The main role of adipose tissue is to store energy in the form of lipids and those lipids are main stored in the sites of mesenteric fat, muscle and liver in fish (Sheridan, 1988). In Atlantic salmon, the visceral adipose tissue and the adipose tissue named myosepta, a connective tissue that separates the muscle sheets, allowing for a continuous muscle structure (Zhol et al., 1995) are primary lipids storage sites (Jezierska et al., 1982; Morgan et al., 2002; Rowe et al., 1991). In Atlantic salmon visceral or abdominal adipose tissue is located inside the abdominal cavity, packed between the intestine, stomach and live. The location of different types of adipose tissues is shown in Fig.1. Subcutaneous adipose tissue (SC) is located around the body of the fish and is more predominant in dorsal and ventral area (Weil et al., 2013). Dorsal subcutaneous adipose tissue (SCD) is situated in the region between the head and the dorsal fin. And as one of the components of the belly flaps, ventral subcutaneous adipose tissue (SCVe) is localized in the abdomen of fish that represents the part of the flesh that hangs under the ribs.

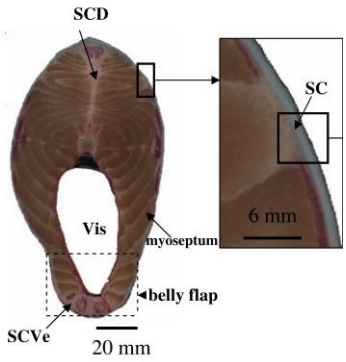

Fig. 1 Representation of a rainbow trout cutlet (situated in front of the dorsal fin). Vis location of the visceral adipose tissue. SCD, SCVe subcutaneous adipose tissues in the dorsal and ventral positions, respectively. SC subcutaneous adipose tissue. (Figure is modified from (Weil et al., 2013))

There are two different types of adipose tissues: white adipose tissue (WAT) which stores energy and brown adipose tissue (BAT) which generates heat of the body. Brown fat or brown adipose tissue is a specialized form of adipose tissue functioning as thermogenesis in human other mammals. Through the expression of uncoupling protein 1, brown fat generates heat by "uncoupling" the respiratory chain of oxidative phosphorylation within mitochondria(Cannon & Nedergaard, 2004). Compare with brown fat, white fat is considered the main energy storage tissue of the organism by depositing the excess energy in the form of triglycerides (TAGs) in adipocytes and can mobilize this energy when starving (Bernlohr et al., 2002). As the major constituent of adipose tissue in Atlantic salmon, adipocytes wildly distribute in visceral adipose tissue, subcutaneous fat layer, belly flap, and myosepta (Zhou et al., 1996). When energy is requested, adipocytes break the TAG into glycerol and acids which are used in fatty acids oxidation to create energy.

Adipose tissue is a sublet and complex ecological cell milieu since it contains the heterogeneous cell population (Fig.2) which exists a large pool of adipocytes and its progenitors with the ability to regenerate new adipocytes. Besides, the endothelial cells and pericyte cells are located inside and outside the blood vessel containing hematopoietic cell populations (erythrocytes, lymphocytes, monocytes, etc). There is also a number of stromal progenitor/stem cells that can be easily expanded *in vitro* and have the potential to create diverse lineages of cells. The extracellular matrix (ECM) is a three-dimensional network consisting of extracellular macromolecules and minerals, such as collagen, enzymes, and glycoproteins that provide structural and biochemical support to surrounding cells.

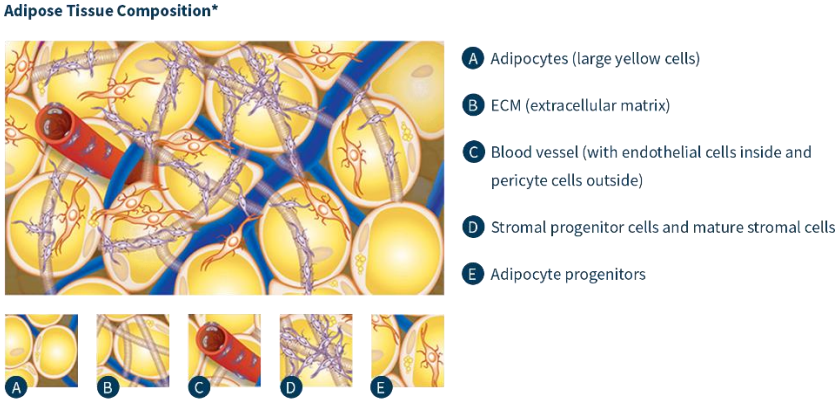

Fig.2 Composition of adipose tissue (Figure modified from https://www.vippng.com/maxp/hxwhwoi/)

2.2 Growth and development of Adipose tissue

The growth of adipose tissue is determined by both hyperplasia (increase in cell numbers) and hypertrophy (increase in cell size). White Adipose tissue possesses the ability to increase its size drastically by hypertrophy without an underlying transformed cellular phenotype (Rajala & Scherer, 2003). Mature adipocyte is among the biggest cell of body and can still increase size by accumulating more TAGs (Bernlohr et al., 2002). And it was demonstrated that human adipocytes can change about 20-fold in diameter and several thousand-fold in volume (Björnheden et al., 2004).

The development of adipose tissue in mammals is the continuous process in which pluripotent mesenchymal stem cells (MSCs) proliferate and differentiate into mature adipocytes (Wei et al., 2008). To understanding the process that fish progenitor cells differentiate and mature to adipocyte, primary cell culture as an effective method *in vitro* provides us a good view to understand it. Primary culture is *ex vitro* culture of cells freshly obtained from multicellular organism. Cells that are cultivated directly from animal tissues are called “primary cells”. Compared with the immortalized cell lines, primary cells in culture provide a more relevant model for *in vivo* situation to the cellular development and functions (Todorcevic et al., 2009). However, primary cells require adequate substrate and unique growth conditions to thrive and after a certain number of divisions they acquire a senescent phenotype, leading to irreversible cell cycle arrest (Campisi & d'Adda di Fagagna, 2007). According to the differentiated extent of primary cells, they can be kept in culture for different period. Fully differentiated primary cells can only have a limited life span (days to weeks), while unspecialized primary cell can be kept in culture for longer periods.

2.2.1 Origin of adipocytes precursors

Stem cells are characterized by the ability to renew themselves through mitotic cell divisions and the capability to differentiate between a variety of cell lineages. The main feature of stem cells is that can differentiate into different cell types, which is to be either totipotent, pluripotent, or multipotent. In comparison with totipotent stem cells that can differentiate into any kind of cell, pluripotent stem cells give rise to various cell types but not to germ cells, and multipotent cells can only differentiate into the limited cell types (Škugor, 2009).

Mesenchymal stem cells (MSCs) are widely used in research due to their easy availability and simple requirements for in vitro expansion and genetic manipulation. In vitro utilizing the physical property of adhering to the plastic surface, different mesenchymal stem populations are isolated (Fig.3). With special

conditions, MSCs possess the vast proliferative potential and the capability of clonally regenerating and developing differentiated progeny.

In mammals, the development of visceral adipose is completed by pluripotent mesenchymal stem cells (MSCs) that proliferate and differentiate into adipocytes throughout life. The plasticity of MSCs has been proved by recent studies. (Casteilla & Dani, 2006) proposed that preadipocytes, osteoblasts, chondrocytes, and myocytes share a common precursor (MSCs). From many mammalian species, in vitro aSVF are readily induced into serval mesenchymal cell lines with the induction of specific growth and nutritional effectors, which including adipogenic (Farrington-Rock et al., 2004; Wei et al., 2008), osteogenic (Doherty et al., 1998), chondrogenic (Farrington-Rock et al., 2004) and myogenic cell lineage (Mizuno et al., 2002) (Fig.3). This pluripotent function ability has also been proved in Atlantic salmon that MSCs from the white muscle of Atlantic salmon can differentiate to osteogenic lineage (Ytteborg et al., 2010).

Studies suggested that MSCs originate from multipotent pericytes residing in blood vessel walls (Traktuev et al., 2008; Zannettino et al., 2008). (Gimble et al., 2007) demonstrated that the smooth-muscle-like pericytes are laid over junctions of endothelial cells. (da Silva Meirelles et al., 2008) suggested that a pericyte should be considered as a MSC and is activated once liberated from the endothelial cells. In rat and human organ, the differentiation maker of smooth muscle cells, α-smooth muscle actin, was demonstrated in the cytoplasm of pericytes (Skalli et al., 1989). The similar result was found first in fish species that the pericyte maker transgelin was expressed in aSVF which is derived from adipose tissue of Atlantic salmon (Todorčević et al., 2010). These findings both indicate that the origin of adipocyte precursor is pericytes.

2.2.2 Lineage determination

Lineage determination involves the commitment of pluripotent stem cells to adipocyte lineage. After this phase, it is difficult to distinguish the morphological differences between the committed preadipocytes and their precursor cells. And those committed preadipocytes also have lost the potential of differentiating into other cell types, which is also the reason why this stage is named determination. The committed preadipocytes first undergo the growth arrest process, which is associated with contact inhibition at the confluence (Todorcevic et al., 2009). Subsequently, by the induction of hormones, preadipocytes re-entry the cell cycle and pass through a limited number of cell division events (Gregoire et al., 1998; Otto & Lane, 2005). The process that preadipocytes re-entry the cell cycle is known as the “clonal expansion” phase, which is essential for the optimal conversion of preadipocytes to mature adipocytes (Gregoire et al., 1998;

Gregoire, 2001). While clonal expansion is finished, cells experience growth arrest again and initiate the expression of specific adipogenic genes that will involve the terminal differentiation process of adipocytes.

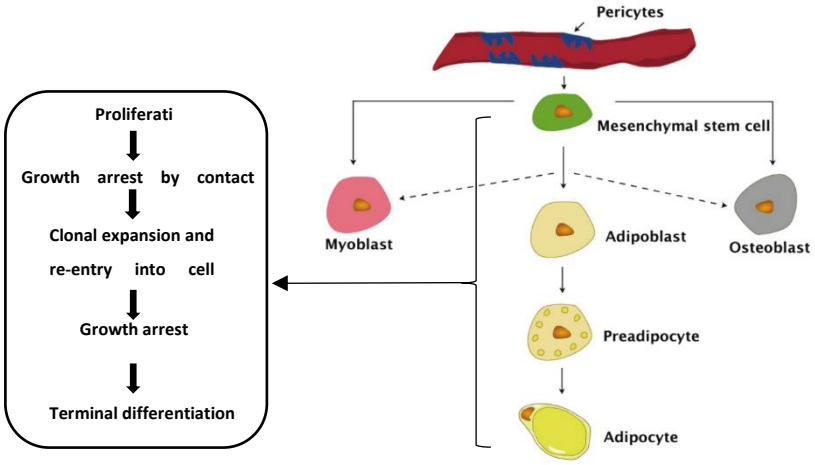

Fig.3 The different stage of adipogenesis and overview of Mesenchymal stem cell differentiating into various cellular lineages. (Figure modified from(Todorcevic et al., 2009))

2.2.3 Terminal differentiation

The second phase is terminal differentiation that preadipocytes convert to mature adipocytes, in which involves the necessary machinery for lipid transport and synthesis, insulin sensitivity and the secretion of adipokines (MacDougald & Rosen, 2006). Recent studies have investigated this phase in three fish species: Atlantic salmon (Todorčević et al., 2008; Todorčević et al., 2010; Vegusdal et al., 2003), red sea beam (Salmerón et al., 2016) and rainbow trout (Bou et al., 2017; Bouraoui et al., 2008).

Adipogenesis is driven by a complex and well-orchestrated signaling cascade that involves regulating the expression and activity of several key transcription factor families. During mammalian and fish adipocyte differentiation, the adipocyte phenotype is recognized by the chronological changes in the expression of numerous genes (Bouraoui et al., 2008; MacDougald & Rosen, 2006; Salmerón et al., 2016; Todorčević et al., 2008; Todorčević et al., 2010). Members of several transcription factor families paly the significant role in this process for both fish and mammals including CCAAT/enhancer-binding proteins (C/EBPs), C/EBPα, C/EBPβ, C/EBPδ), peroxisome proliferator-activated receptor (PPARγ) and the adipocyte determination

and differentiation-dependent factor-1/sterol regulatory element-binding protein-1c (Gregoire et al., 1998; Ntambi & Young-Cheul, 2000; Rangwala & Lazar, 2000; Rosen et al., 2000).

In addition to the expression of specific transcription factors, the specific lineage commitment of MSCs is largely influenced by culture conditions in which the extracellular matrix environment, cell adhesion molecule expressions and growth factors altogether exert crucial effects (Liu et al., 2009).

2.3 Lipid metabolism in adipocytes

As a key organ in the regulation of energy metabolism, adipose tissue stores fatty acids (FAs) in form of TAGs, in which the glycerol is esterified with three FAs. The lipid or fatty droplets formed by TAGs exclude water and has been packed densely and efficiently. This high efficiency of energy storage in fat is an important reason that animals store most of their energy as fats, and only a small amount of energy as carbohydrates (Bernlohr et al., 2002).

2.3.1 Fatty acid uptake

For fish species, the mechanism that FAs are taken up into adipocytes is not as fully studied as in mammals. In mammals, the transportation of FAs into adipocytes is predominantly mediated by proteins such as, plasma membrane fatty acid binding protein (FABP) (Potter et al., 1987), fatty acid transport protein (FATP) (Schaffer & Lodish, 1994), fatty acid translocase (Abumrad et al., 1993) and caveolin-1(Trigatti et al., 1999). FAs firstly are bound by translocase and then are transported into cell with the mediation of FATPs. After entering cells, FAs are acylated by acyl-CoA binding protein and subsequently bound by FABPs to prevent rapid efflux. Inside the adipocytes, FABPs are bonding with free fatty acids and shuttles FAs between the plasma membrane and intracellular membranes or metabolic compartments.

In Atlantic salmon, the expression of FATP1 and scavenger receptor class B type I that was thought may be involved in the lipids uptake from diets and was identified in salmon intestine (Kleveland et al., 2006), are confirmed (Todorčević et al., 2008). The expression pattern of the adipose tissue type FABP (FABP11) in Atlantic salmon has recently been described (Torstensen et al., 2009), and the significant increase in FABP11 expression that occurs in the mature adipocytes is considered as a late maker of adipocyte differentiation (Bernlohr et al., 2002).

2.3.2 Triacylglycerol synthesis and lipid droplet formation

The fate of intracellular FAs depends on the energy status of organism. With excessive energy intake, the abundant calories in form of FFAs will be stored in the form of TAG primarily in adipose tissue (Bernlohr et al., 2002). The main source of glycerol backbone in TAG is glycerol-3-phosphate which is produced by the catabolism of glucose via glycolysis. However, a large proportion of glycerol also seem to be produced in the other metabolic pathway known as "glyceroneogenesis" in which pyruvate functions as an intermediate (Ballard et al., 1967). It has been suggested that this pathway is important in the situation of no sufficient glucose supply (Hemre et al., 2002). In salmonids, the low carbohydrate proportion in diets may explain the formation of glycerol-3-phosphate from substrates other than glucose. With the substantial amounts of FFAs entering bloodstream, the rapid clearance of FFAs from bloodstream is an important step to reduce the lipotoxicity (Bernlohr et al., 2002). And such a strategy may enable the better adjustment of exact cellular demand (Todorčević et al., 2010).

Lipid droplets, also termed "fat globules", "oil bodies", "lipid particles" and "adiposomes", consists of a neutral lipid core (primarily TAG and/or cholesteryl ester), a phospholipid monolayer, and lipid droplet-associated proteins (Brown, 2001; Tauchi-Sato et al., 2002). The mature lipid droplet occupies the major portion of the cytoplasm in both mammalian and fish white adipose tissue (Fig.4).

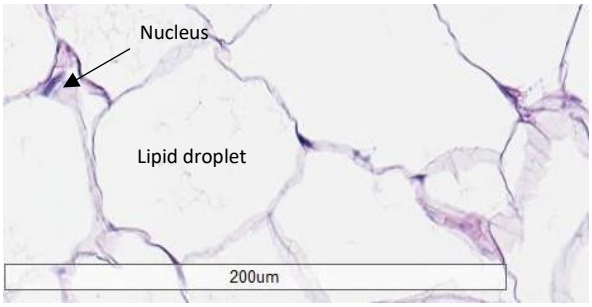

Fig.4 Microscopy of mature Atlantic salmon adipocyte in vivo. The cytoplasm is completely filled with a lipid droplet. The nucleus and cytoplasm are "squeezed" between the lipid droplet and the cell membrane.

Lipid droplet are formed within two different environmental conditions. First, in response to abundant exogenous lipids, cells accumulate lipids droplets and, in this case, are directed towards generating energy and forming membrane (Murphy, 2001). Within many kinds of cellular stress including inflammation and apoptosis, cells induce lipid droplets as well (Gubern et al., 2009). Although how the lipids droplets form has not been fully investigated, many studies support the hypothesis that lipid droplets form in ER. Neutral

lipids are synthesized between the two leaflets of the ER membrane and then the formed lipid droplets bud off into the cytosol together with part of the cytosolic lipid monolayer of the ER (Murphy & Vance, 1999).

2.3.3 β-oxidation of fatty acids

When energy is demanded TAGs in adipocytes are hydrolyzed into glycerol and FFAs that are dominantly transported to other organs such as the liver, muscles and the heat for β-oxidation. β-oxidation is the essential process by which FAs are catabolized through the sequential removal of two-carbon units from the acyl chain (Schulz, 2002).

There is the particularly high capacity for β-oxidation of FAs within the liver (Crockett & Sidell, 1993), red muscle (FrØyland et al., 2000) and the heart (Bilinski & Jonas, 1970). Although the knowledge about β-oxidation in adipose tissue is little known. (Maassen et al., 2007) has shown that the mammalian visceral adipose tissue is able to oxidize substantial amounts of FAs over a long period by mitochondrial β-oxidation. The capacity for β-oxidation of Atlantic salmon adipocytes both *in vivo* and *in vitro* has also been validated (Todorčević et al., 2008; Todorčević et al., 2010), which is depending on the developmental stage and the diet.

The β-oxidation of FAs mainly occurs in the mitochondria. Mitochondrial β-oxidation occurs in the inner mitochondrial space (Eaton, 2002). In fish as in mammals, short-chain FAs (shorter than C6) and medium-chain FAs (C6-C12) can transverse the mitochondrial membrane without the mediation of the carry-transporter. However, the mitochondrial entry for long-chain FAs (C14-C20) must be associated with carnitine, which is a reaction catalyzed by the enzyme carnitine palmitoyl-transferase (CPT) I (Eaton, 2002). Generally, this reaction is considered as the rate-limiting step in the regulation of mitochondrial β-oxidation, namely the conversion of acyl-CoA to acyl-carnitine. Acyl-carnitine is then transported across the inner mitochondrial membrane in exchange for free carnitine molecules, and the acyl-carnitine esters are converted back to fatty acyl-CoA in a reaction catalyzed by CPTII and then β-oxidized. (Todorčević et al., 2008) have found both CTPI and CTPII in Atlantic salmon and have also confirmed the expression of CTPII in adipocytes. Indicate that, except for a lower production of CO^2 (Hagve et al., 1986), β-oxidation reaction in fish is the same as that in mammals.

2.4 Adipose tissue function in immunity

As mentioned before, adipose tissue functions in buffering daily influx of nutrients and maintaining the energy homeostasis of organism. As a place for the long-term storage of lipids, adipose tissue also plays a role in protecting the cell or the whole organism against the lipotoxicity caused by free fatty acids (FFAs) (Slawik & Vidal-Puig, 2007). Previously adipose tissue was considered as a simple, static and lipid-storage tissue. Today, through the secretion of numerous adipokines, adipose tissue is considered to be an active endocrine and secretory organ with multiple functions in metabolic processes. Visceral adipose tissue in mammals produces more than 50 cytokines, termed "adipokines" (Lago et al., 2007) Fig.5. that are biologically active substance with signaling properties. These adipokines are classified according to their functionals roles: appetite and energy balance, immunity, insulin sensitivity, blood pressure regulation, lipid metabolism and homeostasis (Todorcevic et al., 2009) Fig.5.

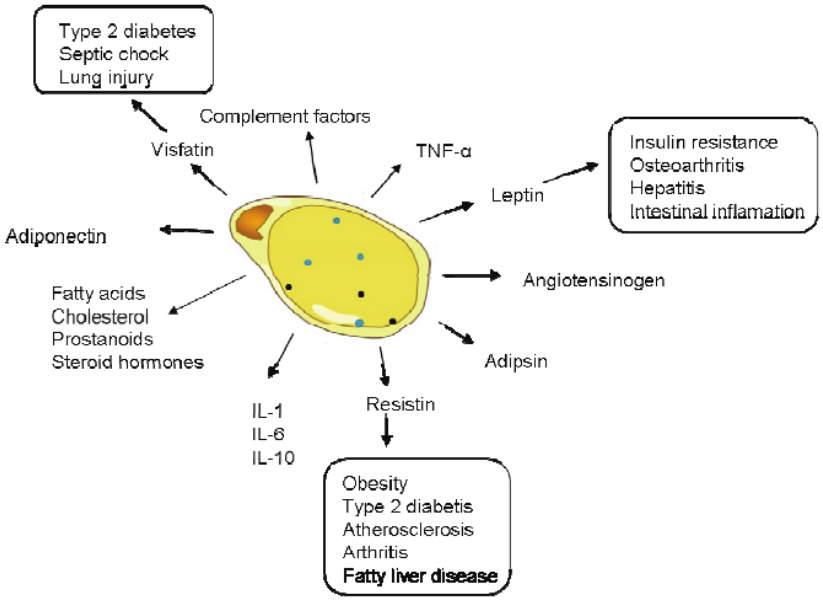

Fig.5 Adipose tissue as an endocrine organ. The overviews of functions of white adipose in mammals including the synthesis and secretion of adipokines, and the uptake, storage and synthesis of lipids. It is also a source of pro-inflammatory factors that modulate the inflammatory response. IL –interleukin; TNF- tumor necrosis factor. (Figure modified from (Todorcevic et al., 2009))

Adipokines secreted by adipose tissue are biological active substance with signaling properties. In mammalian, more than 50 adipokines are identified and the classification is made according to different function role (Lago et al., 2007). Some adipokines may act in the vicinity of their production site in the

autocrine and paracrine network. There still are some other (Elmquist et al., 1999) specific hormones can be secreted into circulation. These factors fulfill important endocrine functions in distant target organs, such as brain or immune organs.

2.4.1 Adipokine secretion

Adiponectin (also referred to as GBP-28, apM1, AdipoQ and Acrp30) is a protein hormone and adipokine that is produced primarily in adipose tissue. The exist of adiponectin has been accompanied by a reduction in plasma glucose and an increase in insulin sensitivity. It has been shown that the concentration of plasma adiponectin correlates negatively with glucose, insulin, and triglyceride levels, and positively with high-density lipoprotein-cholesterol levels and insulin-stimulated glucose disposal (Díez & Iglesias, 2003). Adiponectin increases insulin sensitivity by increasing tissue fat oxidation, resulting in reduced circulating fatty acid levels and reduced intracellular triglyceride contents in liver and muscle (Díez & Iglesias, 2003). This protein also suppresses the cytokine production from macrophages, thus inhibiting the inflammatory processes that occur during the early phases of atherosclerosis.

Adipsin, also known as Factor D, is one of major proteins of adipose cells. Its role is to cleave its specific substrate, factor B, in a Mg^{++}-dependent complex with C3(H2O) or C3b to produce the alternative pathway C3 convertases (C3(H_2O)Bb or C3bBb). In the alternative pathway, factor D is a critical and rate-limiting variable. Besides, it is involved in the amplification loop, which plays an important role in the responses elicited by complement classical and lectin pathways (Podos et al., 2018).

The discovery of leptin, is one of the most important adipose derived hormones, added a new dimension to understand the adipose tissue function in mammals. It was demonstrated that adipocytes not only serve to store energy but directly influence the whole-body energy homeostasis through emitting signals to regulate nutrients uptake and energy expenditure (Zhang et al., 1994). (Vegusdal et al., 2003) firstly found leptin expression in fish species and it is suggested that leptin has the similar function in fish as it has in mammals. Now, it is recognized that adipose tissue plays a significant role in the complex autocrine, paracrine and endocrine network and that it involves in the regulation of variety of diverse biological functions (Todorcevic et al., 2009).

Interleukins (ILs) are a group of cytokines that were first seen to be expressed by white blood cells (leukocytes). The function of immune system largely depends on ILs. Interleukin 1 alpha and interleukin 1 beta (IL1 α and IL1 β) mainly participate in the regulation of immune responses, inflammatory reactions,

and hematopoiesis (Sims et al., 1988). Interleukin 6 (IL6), also referred to as B-cell stimulatory factor-2 (BSF-2) and interferon beta-2, acts as both a pro-inflammatory cytokine and an anti-inflammatory myokine. For instance, smooth muscle cells in many blood vessels produce IL-6 as a pro-inflammatory cytokine (contributors, 2021c). IL-6 function as an anti-inflammatory myokine, which is mediated through its inhibitory effects on TNF- α and IL-1, and activation of IL-1ra and IL-10.

2.4.2 TNF related cell signaling

Tumor necrosis factor (TNF, cachexin, or cachectin), often called tumor necrosis factor alpha or TNF-α, is a cytokine that is primarily used in immune system. There are two receptors existed in TNF cell signaling: TNFR1 (TNF receptor type 1) and TNFR2 (TNF receptor type 2). TNF1 signaling tends to be pro-inflammatory and apoptotic, whereas TNFR2 signaling is anti-inflammatory and promotes cell proliferation (Gough & Myles, 2020; Heir & Stellwagen, 2020).

TNF can bind two receptors, TNFR1 and TNFR2. The most information regarding TNF signaling is derived from TNFR1 since TNFR2 has not intracellular death domain. With the contact with their ligand, a conformational change occurs in TNF receptors, resulting in the dissociation of the inhibitory protein SODD from the intracellular death domain. This dissociation enables the TNFR-1-associated death domain protein TRADD to bind to the death domain, which serves as a platform for subsequent protein binding. There are three pathways are demonstrated following the TRADD binding.

Activation of NF-κB: TRADD recruits the serine-threonine kinase RIPK1 and two ubiquitin ligases: TRAF2 and clAP1. TRAF2 in turn recruits the multicomponent protein kinase IKK complex, enabling the RIPK1 to activate it. RIPK1 is then polyubiquitinated, allowing NEMO (Necrosis Factor-kappa-B essential modulator) to bind to the IKK complex. TAB2 and TAB3 adaptor proteins recruit TAK1 or MEKK3 to activate IKK, which results in the phosphorylation of the NF-κB inhibitors by the activated IKK complex. IκBα is an inhibitory protein that normally binds to NF-κB and inhibits its translocation, which is phosphorylated by IKK and subsequently degraded, releasing NF-κB. NF-κB is a transcription factor that translocates to the nucleus and mediates the transcription and it has been shown to involve in both necroptosis and cell survival.

Induction of death signaling: TNR1 is involved in the death signaling like necroptosis and apoptosis with the function of death domain. In cell death signaling, once the assembly of the TNF ligand to its the TNFR starts, the intracellular domain of TNFR starts the recruitment of the adaptor TNFR-1-associated death

domain protein TRADD, which recruits RIPK1 and two ubiquitin ligases: TRAF2 and clAP1. This complex is called the TNFR-1 complex I. However, its death-inducing capability is not stronger compared to other family members (such as Fas). The fas receptor also known as Apo-1 or CD95, is a transmembrane protein of the TNF family which binds the Fas ligand (FasL). The interaction between Fas and FasL results in the formation of the death-inducing signaling complex (DISC), which contains the Fas-associated death domain protein (FADD), caspase-8 and caspase-10. Processed caspase-8 directly activates other members of the caspase family like caspase-3 that triggers the execution of apoptosis of the cell. Besides, the Fas-DISC can increase the release of proapoptotic factors like cytochrome 3 from mitochondria and the amplified activation of caspase-8.

Activation of the MAPK pathways: RAF2 activates the JNK-inducing upstream kinases, which then activates JNK by phosphorylation. JNK translocates to the nucleus and activates transcription factors such as c-Jun and ATF2. The JNK pathway is involved in cell differentiation, proliferation, and is generally pro-apoptotic.

2.4.3 Complement system

The complement system, also known as complement cascade, is a part of the immune system that stimulates phagocytes to clear foreign and damaged material, attract additional phagocytes, and activate the cell-killing membrane attack complex. There are three biochemical pathways activating the complement system: the classical complement pathway, the alternative complement pathway, and the lectin pathway (Fig.6).

The classical pathway is triggered by activation of the C1-complex, or *C1qr2s2*, that is composed of 1 molecule of C1q, 2 molecules of C1r and 2 molecules of C1s. This occurs when C1q binds to IgM or IgG complexed bound to antigens. The C1r2s2 component splits C4 and then C2, producing C4a, C4b, C2a, and C2b. C4b and C2b bind to form the classical pathway C3-convertase (C4b2b complex) that promotes the cleavage of C3 into C3a and C3b. C3b later combines with C4b2b to make C5 convertase (C4b2b3b complex).

The alternative pathway is continuously activated at a low level as a result of spontaneous C3 hydrolysis due to the breakdown of the internal thioester bond (C3 is mildly unstable in aqueous environment). C3b is generated from C3 by a C3 convertase enzyme, which can be is rapidly inactivated by factor H and factor I. The C3b can bind factor B to form C3bB complex that will be cleaved into Ba and Bb in the presence of factor D. Bb will remain associated with C3b to form C3bBb, which is the alternative pathway C3

convertase (Rooijakkers et al., 2009). The C3bBb complex is stabilized by binding oligomers of factor P (properdin), C3bBbP, that then acts enzymatically to cleave more C3 and recruits more B, D and P activity and greatly amplifies the complement activation. Once the alternative C3 convertase enzyme is formed on a pathogen or cell surface, it binds covalently another C3b to form C3bBbC3bP, the C5 convertase that then cleaves C5 to C5a and C5b. The C5b then recruits and assembles C6, C7, C8 and multiple C9 molecules to assemble the membrane attack complex.

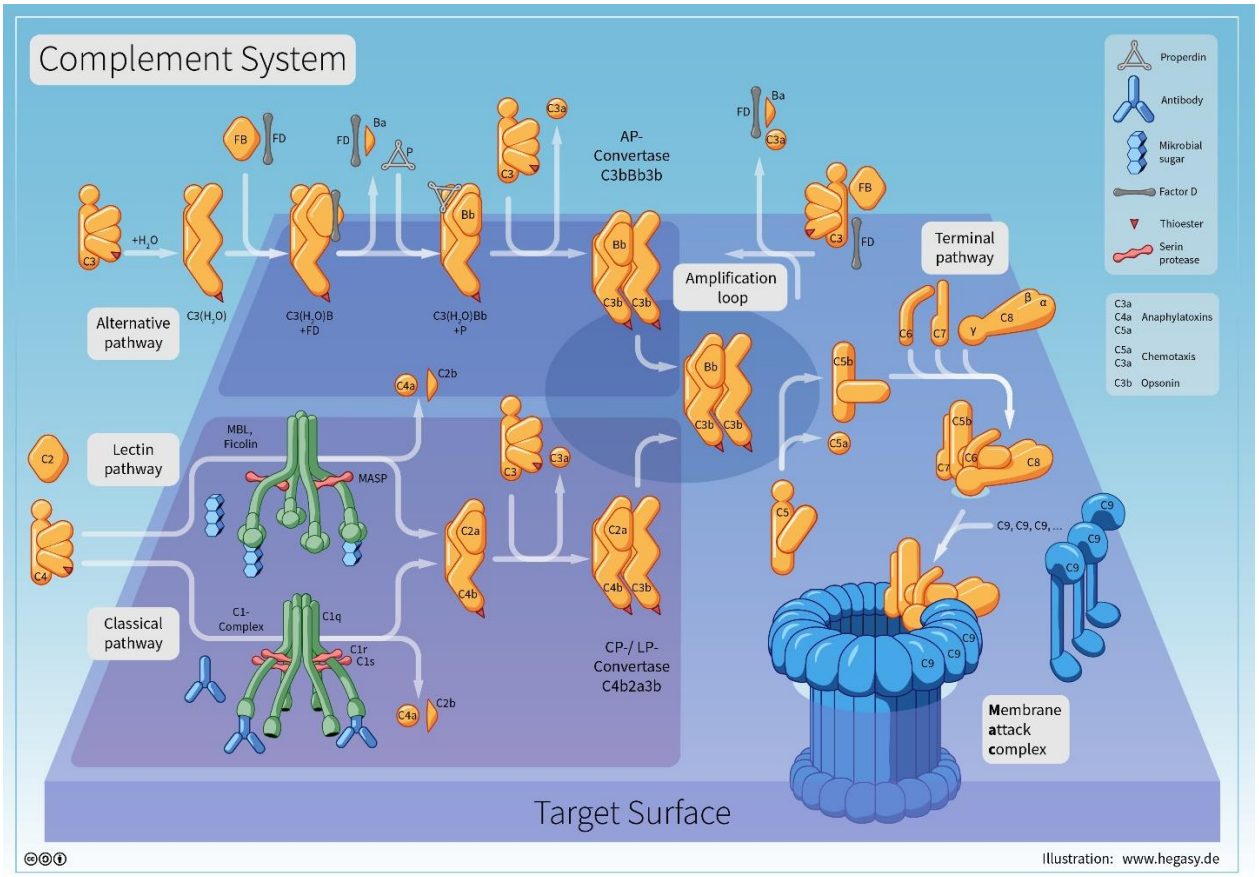

Fig.6 The overview of Complement System (Figure captured from https://en.wikipedia.org/wiki/File:09_Hegasy_Complement_System_Wiki_EN_CCBYSA.png)

The lectin pathway is homologous to the classical pathway. This pathway is activated by binding of mannose-binding lectin and ficolins to mannose residues on the pathogen surface, which activates the MBL-associated serine proteases, MASP-1, and MASP-2 (very similar to C1r and C1s, respectively). Such a complex can then split C4 into C4a and C4b and C2 into C2a and C2b. C4b and C2b then bind together to form the classical C3-convertase, as in the classical pathway.

2.4.4 Intimate relationship between adipocytes and macrophages

It has been validated that there is a complex relationship between adipose tissue and immune system due to a large amount of relative adipokines secretion described in the last section. And some researchers consider adipose tissue to be an ancestral immune organ (Caspar-Bauguil et al., 2005).

As mentioned early, visceral adipose tissue, as a heterogeneous organ, is composed of many cell types. The close interaction between adipocytes and macrophages implicates an essential effect in determining adipose biology and regulating adipose tissue homeostasis. Many initially macrophage-specific functions have now been described in adipocytes and vice versa Fig.7. In normal conditions, adipocytes function in storing lipids in form of TAGs and are responsible for metabolic homeostasis, while macrophages are function as pathogen sensor and are involved in the initiation of inflammatory response. However, each of these cells has the capacity to perform both functions. In obesity, adipose tissue become inflamed, both through infiltration of adipose tissue by macrophages and as a result of adipocytes themselves become the producers of inflammatory cytokines.

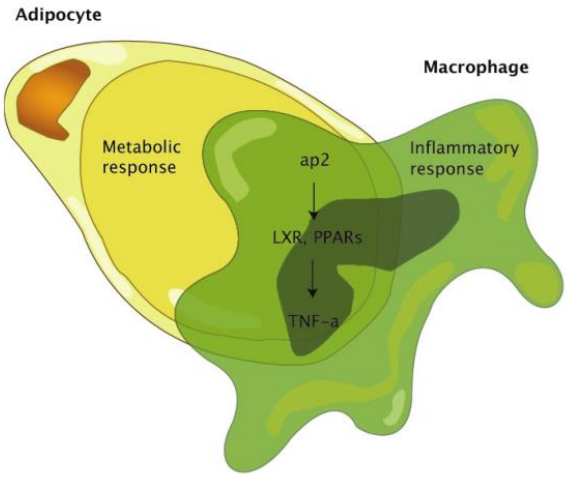

Fig.7 Integration of metabolic and immune responses in adipocytes and macrophages through shared mechanisms. Adipocytes and macrophages share common features such as expression of cytokines, FABPs, nuclear hormone receptors, and many other factors. adipocyte/macrophage FABPs modulate both lipid accumulation in adipocytes and cholesterol accumulation in macrophages (Figure is captured from (Todorcevic et al., 2009)). PPARγ and LXR pathways oppose inflammation and promote cholesterol efflux from macrophages and lipid storage in adipocytes. aP2-adipocyte fatty acid binding protein; LXR-liver x receptor; PPAR-peroxisome proliferator-activated receptor; TNF-tumor necrosis factor.

(Charrière et al., 2003) indicates that preadipocytes and macrophage share a great number of common features in mammals. By comparing the gene expression profile between adipocyte progenitors and macrophages, showed that preadipocytes have the capacity to trans-differentiate into macrophages. Similar results have also been demonstrated in Atlantic salmon preadipocytes (Škugor, 2009). Undoubtedly, adipose precursor cells exhibit a high degree of plasticity. Besides, recent studies have shown that macrophages and adipocytes have many similarities in the expression of cytokines. For instance, macrophages express many "adipocyte" gene products such as FABPs and PPARγ (Makowski et al., 2001; Tontonoz et al., 1998), while adipocytes express many "macrophage" gene products such as TNFα, IL-6, and matrix metalloproteinases (Bouloumié et al., 2001; Gökhan et al., 1993).

In summary, these observations have implied the plasticity of adipose precursor cells and emphasized the close relationship between innate immunity and adipose tissues.

2.5 Method for studies of adipose tissue morphology

Histology is a study of microscopic anatomy of cells and tissues. By sectioning and staining cells or tissues, the improved microscopic structures under microscopes are observed. There are three major steps when processing tissue for histology: fixation, embedding and staining.

After being collected, sample fixation is an essential procedure to prevent samples from autolysis or putrefaction. It terminates ongoing biochemical reactions in the cells and also increase the mechanical strength of the tissue. In tissues, the crosslinking reaction happens between proteins, in which adjacent lipids hold them firmly and lipids molecules are fixed in the original location. However, the adipose tissue is predominantly composed of lipids, which increase difficulty of fixation in adipose tissue. The conventional fixatives such as formaldehyde or paraformaldehyde (PFA) are normally used for the preservation of biological samples. It shows strong capacity to prolong the decaying process of dead organism (Mao & Universitetet for miljø- og biovitenskap Institutt for husdyr- og, 2012). The most other fixatives including alcohols and glutaraldehyde are deficient in preserving lipids due to the extraction lipids during fixation. Besides, due to the low ability of diffusion in tissue sections, glutaraldehyde does not show good fixation results of lipids especially in thick sections (Mao & Universitetet for miljø- og biovitenskap Institutt for husdyr- og, 2012). Thus, this fixative is not ideal for immunohistochemistry staining. Although the chemical fixing method (most common fixative is 10% neutral buffered formalin light microscopy) normally causes the degradation of some molecules like mRNA and DNA, it functions well for the fixation of intracellular lipids and nerve tissues.

Embedding is a process that consists of casting and blocking tissue samples for the subsequent sectioning. Maintaining the native morphology of tissues is the main purpose in embedding procedure. It includes the enclosure of the tissue in the infiltration medium and the medium solidification. Specimens normally are taken through a series of water/alcohol mixtures to full alcohol and then through a clearant like xylene (HistoClear) or substitutes, making sample tissues transparent, and finally melted paraffin. Formalin-fixated paraffin embedded tissues show bad preservation for RNA and some antigens. However, this method presents a good morphology of samples (Finke et al., 1993).

Staining, as an assistive technology, is used to enhance contrast in microscopic image. By adding class specific (DNA, protein, lipids, carbohydrates etc.) dyes, we are able to qualify or quantify the specific compounds (Ugye, 2010). Staining not only make the cells to be more easily seen but allows their morphology e.g., size and shape to be visualized more easily. The staining process normally involves immersing the sample in a solution of a dye, followed by rinsing and observation (Ugye, 2010). The use of mordant, a chemical compound reacting with the stain, is required for many dyes. However, the reaction between mordant and the stain will form an insoluble colored precipitate that is hard to wash away even with the excess dye solution.

There are already many stains as fluorescent imaging tool used in histology. Phalloidin, a rigid bicyclic heptapeptide, functions by binding and stabilizing filamentous action (F-actin), the element of microfilaments, and effectively prevents the depolymerization of actin fiber (contributors, 2021d). Due to this tight and selective binding ability, fluorescent derivatives of phalloidin have been used in localizing actin filaments in living or fixed cells as well as for visualizing individual actin filaments *in vitro* (Cooper, 1987). DAPI or 4’,6-diamidino-2-phentlindole, can strongly binds to adenine-thymine-rich regions in DNA and pass through an intact cell membrane, which is extensively used in fluorescence microscopy. It can be used to stain both live and fixed cells (contributors, 2021a). DAPI has an absorption maximum at a wavelength of 358 nm (ultraviolet) and an emission maximum at 461 nm (blue) when bound to double-stranded DNA. Therefore, DAPI is excited with ultraviolet light and can be detected through a blue/cyan filter (contributors, 2021a).

For cellular lipids staining, LipidTOX neutral lipids stains is considered as more selective and flexible reagents for application in adipogenesis and pathway mapping in comparison to Nile red stain. It shows superior performance over Nile red due to its specificity for neutral lipids, greater signal intensity and lower background levels (Chun et al., 2013). Additionally, (Ramírez-Zacarías et al., 1992) reported that the Oil red O (ORO), as a soluble colorant, can also specifically stain triglycerides and cholesteryl oleate but no

other lipids. However, ORO is fixative based dyes requiring fixation beforehand, which is time consuming and may cause deformation of lipid droplets in adipose tissue (Fukumoto & Fujimoto, 2002). In contrast, cell fixation is not required for LipidTOX, suggesting that LipidTOX can be implied *in vivo*. The ORO stain has been turned out to be very useful for processing large numbers of cell cultures and samples in which the level of adipose differentiation and/or triglycerides accumulation needs to be quantified (Ramírez-Zacarías et al., 1992).

2.6 Cell culture system

For the cell culture system, there already is the culture model of primary preadipocytes that is isolated from the stromal vascular fraction of adipose tissue (aSVF) in Atlantic salmon. It was developed to investigate the commitment of the differentiation process from preadipocytes to adipocytes. Normally, cell culture is treated with a combination of adipogenic effector (Vegusdal et al., 2003). For instance, Dexamethasone (DEX) is used to stimulate the glucocorticoid receptor pathway. 3-isobutyl-1-methylxantine (IBMX) is used to stimulate the cyclic adenosine monophosphate (cAMP)-dependent protein kinase pathway. And triiodothyronine (T3), with the involvement of insulin, is used to enhance the differentiation-linked of lipoprotein lipase gene.

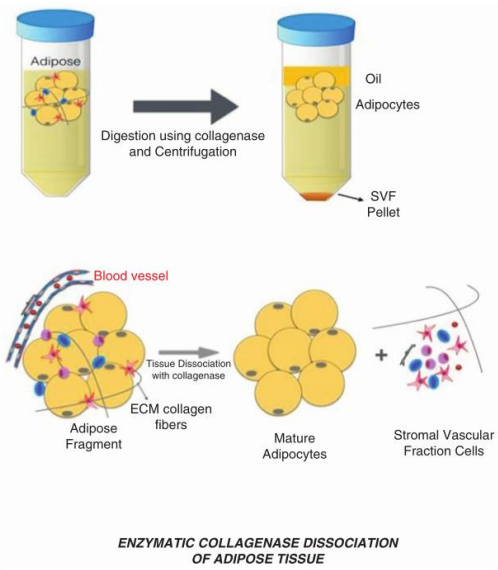

Fig.8 Overview of SVF isolation procedure: adipose digestion in Falcon tubes showing tissue disaggregation, cell release, and concentration of SVF pellet via centrifugation (Figure modified from(Dos-Anjos & Catalán, 2019))

The obtain of aSVF is completed by enzymatic collagenase dissociation, which separates all mature adipocytes (tissue parenchyma) from all other supporting cells (stroma) see Fig.8. The cellular pellet contained the stromal vascular fraction (SVF) that is a very heterogeneous cell population comprised of many different cell types such as blood derived cells (erythrocytes, lymphocytes, monocytes, etc.), endothelial cells, fibroblasts, and other progenitor cells (including mesenchymal stem cells MSCs)(Zimmerlin et al., 2010).

Primary cells used in cell culture system are freshly obtained from multicellular organism. Compared with cell lines, they more closely resemble the *in vivo* situation, and they provide a more relevant system to study the development and functions of the cell since they are the also heterogeneous population of cells like the tissue they originated. However, according to the extent of their differentiated degree, they only have the limited life span (Campisi & d'Adda di Fagagna, 2007). Besides, working with primary cells raises numerous challenges, including the requirement for unique culture supplementations and growth conditions (Škugor, 2009).

2.7 DNA microarray technology

A DNA microarray also commonly known as DNA chip is a collection of microscopic DNA spots attached to a solid surface such as glass, plastic or silicon biochip. DNA microarray is used to measure the expression levels of large numbers of genes simultaneously or genotype multiple regions of a genome. Each DNA spot contains probes that can be a short section of a gene or the other DNA element (contributors, 2021b). These probes are used to hybridize a cDNA sample under high stringency conditions Fig.8 and such a hybridization is usually detected and quantified by detection of fluorophore-, sliver- or chemiluminescence-labeled targets (samples). The overview of the protocol of DNA microarray experiments is explained in Fig .9;10. Within the organisms, genes are transcribed and spliced to produce mature mRNA transcripts. The mRNA is extracted, and reverse transcriptase copies the mRNA into the stable ds-cDNA. In microarrays, the ds-cDNA is fragmented and then fluorescently labeled. The labeled fragments can bind to an ordered array of complementary oligonucleotides. And the measurement of the fluorescent intensity across the array indicates the abundance of the specifically chosen sequence (contributors, 2021b).

The utilization of microarray plays a significant role in gene expression profiling and identification of the genomic response to certain treatments, diseases and developmental stages (contributors, 2021b). For instance, microarray-based gene expression profiling has been used to identify genes whose expression is

changed in response to pathogens by comparing the gene expression in infected to that in uninfected cells or tissues (Adomas et al., 2008).

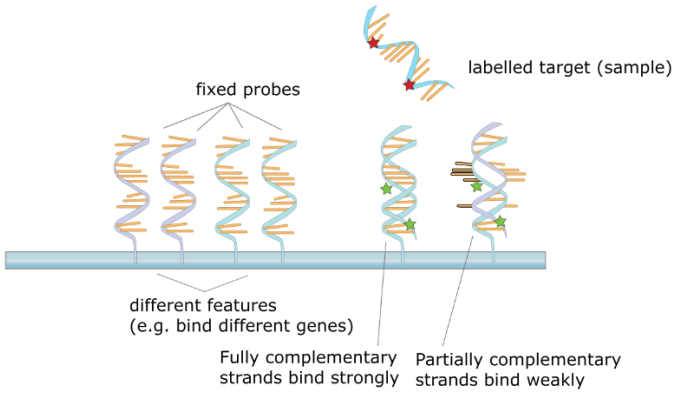

Fig.9 Hybridization of target to probe (Figure captured from https://upload.wikimedia.org/wikipedia/commons/a/a8/NA_hybrid.svg)

However, the advent of microarray experiments creates several specific bioinformatics challenges like the statistical treatment of the data (Data analysis), mapping each probe to the mRNA transcript that it measures (Annotation), etc (contributors, 2021b). Microarray data sets are normally very large, and analytical precision is influenced by a number of variables. The effect of background noise and appropriate normalization of date always challenge the data analysis. Further processing aimed at reducing the dimensionality of the data may aid comprehension and provide a more focused analysis.

The key to the successful interpretation of microarray data is the knowledge of functions of the different expressed gene (Škugor, 2009). Working with non-model organisms is difficult since its functions and regulation have not been fully studied. In the most important salmonids: rainbow trout and Atlantic salmon, the annotation, the crucial step in the sequencing project, of genes is fairly satisfactory. And the gene expression profile during developmental stages (proliferation and differentiation) has been fully understood as well. (Todorčević et al., 2010) has demonstrated the gene expression profile in Atlantic salmon adipose-derived stromo-vascular fraction during differentiation into adipocytes. Besides, Gene expression profile during proliferation and differentiation of rainbow trout adipocyte precursor cells has also been confirmed (Bou et al., 2017). However, there is not much information about the gene expression profiling difference between different adipose tissue in fish.

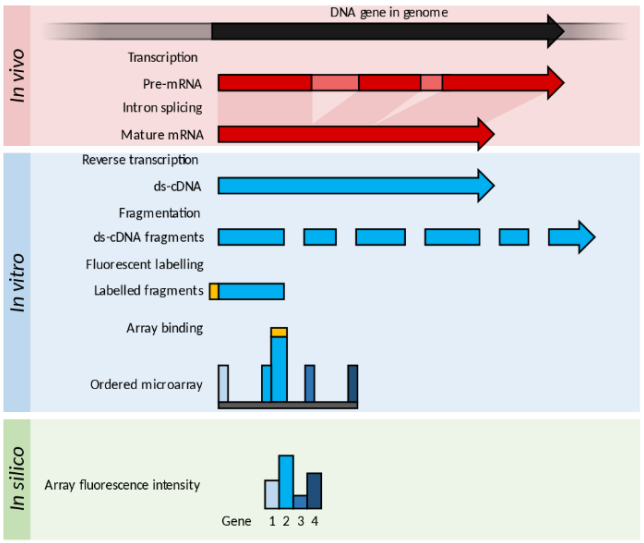

Fig.10 Examples of levels of application of microarrays (Figure captured from https://upload.wikimedia.org/wikipedia/commons/d/d9/Summary_of_RNA_Microarray.svg)

3 Materials and methods

3.1 Materials

Experimental fish from sea cages R and D licenses section parts.

Experimental fish in tanks on land freshwater.

Atlantic salmon (Salmo Salar) used for cell isolations, were farmed in Fiskelaboratoriet og miljøstasjon (Fish Laboratory), NMBU, Norway. They were all smolt between the weight of 1-3kg and were reared in fresh water and fed a commercial diet.

The anesthesia Aqui-S vet. was from Scanvacc (Hvam, Norway). Antibiotics, Nunc™ Cell-Culture Treated Multidishes and Nunc™ Cell-Culture Treated Multidishes were purchased from Thermo Scientific™ (Roskilde, Denmark).

During collagenase digestion, See-saw rockers (SSM4) from Stuart (Staffordshire, ST15 OSA, UK) was used to shake the flask.

Cells in culture were observed in Inverted Laboratory Microscope Leica DM IL LED from Leica Microsystems CMS GmbH (Wetzlar, Germany). Thermo Scientific™ BK 6160 Testing Chambers was used to achieve the required temperature (13℃).

For histology analysis, microscope slides (4951F-001), Shandon Gill 3 Hematoxylin (6765010) and Mounting Media (8310-16) were from Thermo Scientific (MA USA). 5× Zinc-Formalin Concentrate (141) was from Anatech LTD (MI USA) used to fix adipose tissues. 100% and 95% Ethanol were supplied from Decon Labs (PA USA). For samples embedding, cassettes (4135) and metal embedding molds (4124) were from Sakura Finetek USA (CA USA). Acetone (9006-01), Hydrochloric Acid (9535-00) and Xylene (8668-16) were purchased from Avantor Performance Materials (PA USA). CitriSolv (22-143-975) and Coverslips (12-545-F) were from Fischer Scientific (MA USA). Biobond (71304) was from Electron Microscopy Services (PA USA). Paraffin (EM-400) and Eosin Y Alcoholic (3801600) were supplied from Leica Microsystems (Germany). Lithium Carbonate (L4283) was bought from Sigma-Aldrich (MO USA).

For microarray analysis, RNA is extracted by RNeasy® Mini Kit (Qiagen, Valencia, CA, USA) and RNase-free DNase I (Qiagen, Valencia, CA, USA) is used to exclude any contaminating DNA. Spectrophotometry (NanoDrop® ND-1000 Spectrophotometer, NanoDrop Technologies, Wilmington, DE USA) is used to detect the quality of RNA. The fluorescent dyes Cy5-dUTP and Cy3-dUTP (Amersham Pharmacia, Little Chalfont, UK) were incorporated in cDNA using the SuperScript™ Indirect cDNA Labelling System

(Invitrogen, Carlsbad, CA, USA). Labelled cDNA was purified with Microcon YM30 (Millipore,Bedford, MA, USA). Scanning was performed with Axon GenePix 4100A (Molecular Devices, Sunnyvale, CA, USA)

3.2 Methods

3.2.1 Isolation of pre-adipocytes from visceral and subcutaneous adipose tissues (*in vitro*)

Live Fish individuals were chosen randomly from freshwater tanks(3000litres/3m^3) and transferred to transparent plastic bags with filled oxgenated water from Fiskelaboratoriet og miljøstasjon (Aqui-S vet. (3ml/L) were added to the water in order to calm down the fish during transportation to Nofima laboratory). After obtaining the fish, fishes were anesthetized again in fresh-water tank with Aqui-S vet. (3ml/L) for 5 minutes. Then the gill arch was cut to bleed out the fish. After bleeding for 2-3 minutes, the fish was killed by a blow to the head.

Isolation from visceral fat depot:

The visceral pre-adipocytes were obtained from abdominal adipose tissues depot of Atlantic salmon (*Salmo Salar*). After the fish was dead, the abdomen was disinfected with 70% ethanol. The abdomen was cut open with the autoclaved scissor to expose the visceral adipose depot and adipose tissues were carefully taken out in order to avoid contamination with intestinal contents (Fig.11).

Fig. 11 The exposed visceral adipose tissue

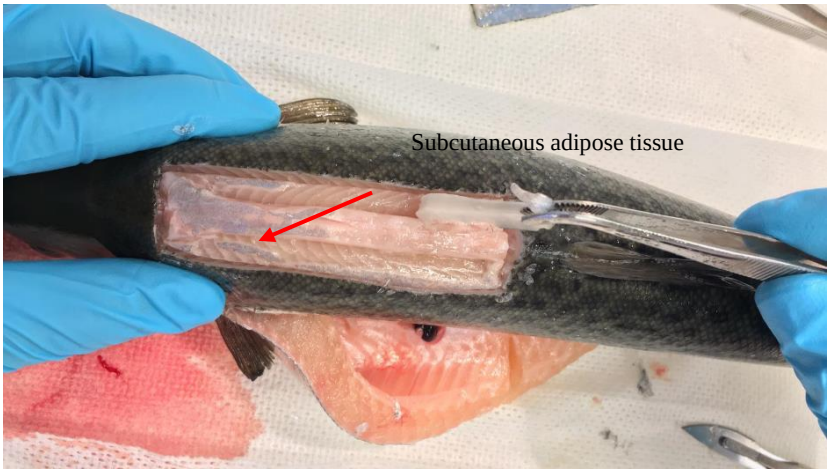

Fig. 12 The exposed subcutaneous adipose tissue

Isolation from subcutaneous adipose depot:

The subcutaneous pre-adipocytes were obtained from dorsal adipose tissues depot beneath the skin around the dorsal fin. Cutting a rectangular-shaped area firstly, then the skin around dorsal fin was teared off by a tweezers to expose the subcutaneous adipose tissue. Then two main strips of tissue were excised (Fig.12).

Both visceral and subcutaneous adipose tissue were processed by the same procedures afterwards. After being excised, the tissue was transferred into the prepared sterile 50ml tube. All those tubes containing approximately 30ml Gibco® L-15 (with GlutaMAX™ supplement) and 1% antibiotics (100 units penicillin, 0.1mg streptomycin and 0.25µg amphotericin B per mL) were weighed and kept on ice in advance. The tissue in each tube was weighed and then centrifuged at 300g (4℃) for 5 minutes to get rid of blood. Then tissues were transferred with an autoclaved spoon to a Petri dish (cell-culture dish). All tissues were manually minced into tiny pieces with two knives (small blood clot was picked up during cutting). The minced tissue was transferred into a cell culture flask (normally 500ml depending on the weight of adipose tissue) with L-15 in the ratio of 1g visceral adipose tissue/ 5ml L-15 supplemented with 0.1% collagenase (1g subcutaneous adipose tissue/ 10ml L-15 supplemented with 0.1% collagenase). The flask was kept on the incubator for one-hour gentle shaking at 13℃ in order to enhance the collagenase digestion.

To remove large cells and undigested tissue, the tissue solution was filtered through 250µm nylon filter into a bottle and filtered again through 100µm filter into the 50 ml tubes. Filters were rinsed with L-15 simultaneously during filtering. After centrifugation (500g, 10mins), the digestion medium and the supernatant containing mature lipid filled adipocytes were removed by aspiration. The precipitate containing pre-adipocytes was re-suspended in 5ml L-15 media with antibiotics (mixture of pencillin, streptomycin and amphotericin B), and precipitates from 3-4 tubes depending on the amount of precipitate

were transferred into a new tube to get higher concentration of cells. The pooled sample was centrifuged (500g, 10mins) again, then the media solution was discarded, and cell pellets were re-suspended with growth media to get cell solution. All aforementioned tools (scissor, blade, tweezers, culture-treated dish, spoon, bottle) were autoclaved in advance.

Two milliliters of cell solution per well were seeded out (day 0) on 6-well plates. Plates had been coated with gelatin on the day before plating, and then plates were washed with PBS three times (2ml per time) when plating. Most cells were attached to the bottom of the plate on the next day after plating. Cells were washed with PBS two times every 2 days, and the 2ml growth media was renewed after washing.

Cells were incubated in an incubator at 13℃ through the whole cultivating period, and they were maintained in growth media containing (L-15, 10%FBS, 2mM L glutamine, 10mM HEPES, and antibiotics) until reaching confluence stage after approximately 1 week. Confluent preadipocytes were firstly differentiated in a differentiation-inducing media containing growth media supplemented with 1µM dexamethasone, 33µM biotin, 10nM triiodothyronine, 17µM panthothenate and 25µM isobutylmethylxanthine, 20 µg/ml insulin and a lipid mixture (5µl/ml; corresponding to 45 mg/ml cholesterol, 100 mg/ml cod liver oil FA (methyl esters)).check in the lab The culture media was changed to a maintenance differentiation medium containing growth medium only supplemented with 5 µl/ml of lipid mixture, and the medium was renewed every 2 days as well until day 15 when cells reached the differentiated stage with the morphology of mature adipocytes.

Table 1 composition of grow media

Media	Components	Concentration
Growth media	DMEM	
	FBS	10%
	HEPES	10mM
	Antibiotic	10ml/L
	Glutamine	2mM
Differentiation media	Dexamethasone	1µM
	Biotin	33µM
	Triiodothyronine	10nM
	Panthothenate	17µM
	Isobutylmethylxanthine	25µM
	Insulin	20 µg/ml
	Lipid mixture*	5µl/ml

*correspondingto 45 mg/ml cholesterol, 100 mg/ml cod liver oil FA

During the cultivating stage the proliferation, differentiation and the accumulation of lipids in adipocytes was evaluated by morphological observation. Cells for microscopy studies were taken from cultures at three different stages: proliferation stage (da y 2 and day4), at confluence (day 7) and differentiation stage (day 9, day 12 and day 15).

3.2.2 Fluorescence staining of intracellular lipid droplets (in vitro)

3.2.2.1 Adipocytes stained with oil red O (ORO) and Coomassie blue Stain

Oil red O (ORO) staining:

Oil red O stocking solution (3.5g/L) was prepared in advance. Oil red O was dissolved in isopropanol as stocking solution and kept in a fume hood overnight. The next morning, the solution was filtered through a Whatman filter. The working solution was made with dissolving the stocking solution with distilled water in the ratio of 3:2 for overnight at 40℃. The next morning, the working solution was filtered as well. After 30 minutes, the solution was filtered again with a 0.2 µm syringe.

The differentiated visceral and subcutaneous adipocytes (day 15) in each well were firstly washed twice with PBS, and the cells were fixed with 10% formalin and incubated for 5 minutes at room temperature. Afterwards, the old formalin was discarded, and fresh formalin was added to incubate the cells at least 1 hour. Then removing the formalin, the cells were washed twice again with PBS. The PBS was subsequently discarded, and let the plate dry a bit. The cells were incubated with the oil red O for 2 hours at room temperature. After removing the oil red O, the cells were washed 3 times with dH_2O. The distribution of intracellular lipids was observed by microscopy, and the images were obtained with a digital camera coupled to the microscopy.

350 µl isopropanol was added in each well to incubate the cells at least for 10 minutes. The solution was pipetted up and down to ensure that all the colors were dissolved in the isopropanol. 100 µl sample which was duplicated to 200 µl in 2 wells was transferred to a 96-well plate. The concentration of lipids in each well was measured by spectrophotometry at 500 nm with two groups of 100% isopropanol as blank group.

Coomassie blue staining (Protein):

After the measurement of lipid concentration, the protein in each well was stained with Coomassie. The Coomassie solution was prepared in advance. 0.04 g Coomassie was added into 100 µl Perchloric acid (3.5 %). The solution was mixed well and then cultivated at room temperature for 24h. Before using this solution, it was filtrated with Whatman filter paper.

The isopropanol solution was discarded, and then the cells were washed twice with dH_2O. Waiting 2 minutes made the plate dry before next processing. 500 µl Coomassie was added to each well, and the cells were incubated for 1 h. Microscopy images were taken after staining as well.

Afterwards, the Coomassie was removed, and 350 µl propylene glycol was added when the plate was dry. The solution was incubated at 60℃ for 1 h. 100 µl sample from each well which was duplicated to 200 µl in 2 wells was transferred to a 96-well plate. The concentration of protein was measured by spectrophotometry at 630 nm with two groups of 100% isopropanol as blank group.

3.2.2.2 Adipocytes stained with LipidTOX

The differentiated adipocytes (day 15) were washed twice with PBS (0.5ml for 12-well plates) and then were fixed with 4% PFA for 30 minutes at room temperature. 4% PFA was diluted from 36.5% PFA with PBS. Afterwards, PFA was removed by pipette, and the cells were washed twice to remove the residual PFA. After washing, the cells were incubated Lipid Tox neutral lipids stain (1:200 in PBS) for 30 minutes in a dark environment. After the incubation, the cells were visualized by using a Leica Paula microscopy, the stained lipid droplets signal was captured under 488 nm with the green fluorescent protein (GFP) filter.

3.2.3 Histology and image analysis for adipose tissues (in vivo)

3.2.3.1 Slides preparation

Belly flap, visceral fat tissue and dorsal fat, 75% (Mix together 750mL 100%EtOH and 250mL dH_2O), 70% ethanol (Mix together 500mL 75%EtOH and 35mL dH_2O) and 1×Zinc-formalin by adding 10mL 5×Zinc-formalin to 40mL dH_2O were prepared in advance.

Visceral fat tissue is in the abdominal cavity around the digestive track. Two subcutaneous fat tissues, dorsal fat layer and belly flap, which is situated around the body of salmon. Before exposing the adipose tissues, the external skin in dorsal and ventral zones was disinfected with 70% ethanol. Visceral fat tissues were carefully cut from the abdominal fat depot. After cutting a rectangular-shaped area in dorsal and ventral skin, the external skin was teared off by a tweezer to expose the subcutaneous adipose tissue underneath. Then stripes of subcutaneous fat tissues were excised. All the samples were incubated in

1×Zinc-formalin overnight at 4℃. After being washed 3 times in sterile PBS, samples were transferred into embedding cassette. The cassette was incubated in 70% ethanol until tissue processing.

For tissue processing, cassette was firstly incubated in 75% ethanol for 30minutes and was transferred in 95% ethanol for 75 minutes incubation. The second incubation was required to repeat a 2nd time with fresh 95% ethanol. Then the cassette was incubated in 100% ethanol for 60 minutes, which this step is repeated a 2nd and 3rd time with fresh 100% ethanol. Subsequently, with 60 minutes incubation in melted paraffin at 60℃, the cassette was transferred to fresh melted paraffin and was incubated overnight at 60℃. Before paraffin embedding, the cassette was transferred again to melted fresh paraffin and was incubated for 60 minutes at 60℃.

The cassette was removed from paraffin. Both the cassette and metal embedding mold were placed on a heating plate set to 60℃. The metal embedding mold is filled 75% with melted paraffin. After being removed from cassette, samples were placed in melted paraffin within the metal embedding mold in the desired orientation. In order to harden the paraffin to maintain the sample orientation, the metal embedding mold was placed on a cold plate set to 0℃ for a few seconds and was placed back on the heating plate set to 60℃. With placing the embedding cassette on the top pf embedding mold, melted paraffin was poured into the embedding cassette to fill the remainder of the embedding mold and the embedding cassette. Then the embedding mold with cassette was immediately transferred to the cold plate waiting until the paraffin had fully hardened. The paraffin block was carefully removed from mold by pulling the attached cassette away from the mold.

Prior to sectioning, coated slides were prepared in advance. Slides were incubated in diluted Biobond (Dilute Biobond 1:50 in acetone) for 5minutes and then in dH_2O for 5 minutes. Slides should be dry before sectioning. Using microtome, 5 µm thick paraffin sections were acquired and were carefully transferred to a water-bath set to 37℃. Each paraffin section was transferred to a slide by submerging the slide into the water bath, placing the slide under the floating section, and raising the slide out of the water such that the section attaches to the slide as it is removed from the water. In order to dry and adhere the tissue sections to the slides, the slides with sectioned adipose tissue were incubated at 40℃ overnight.

Prior to staining, 1% lithium carbonate (saturated) solution by adding 5 g lithium carbonate to 500 mL dH_2O and mixing well, and 70% ethanol by mixing 70 mL 100% ethanol and 30 mL dH_2O were prepared in advance. A HCl-ethanol solution (0.125% HCl in 96.25% ethanol) was prepared by adding 625 µL hydrochloric acid to 62.5 mL 70% ethanol in a 500 mL flask, adding 437 mL 100% ethanol and gently

mixing the solution. Slides were incubated in xylene for 20 seconds with this step repeating 3 more times using fresh xylene each time. Slides then were transferred to 100% ethanol for 20 seconds incubation, which repeated one more time with fresh 100% ethanol. For each time 15 seconds incubation, slides were placed in 95% ethanol and subsequent in dH_2O. Afterwards, the slides were incubated in Shandon Gill 3 Hematoxylin for 15 seconds with this step four more times repeating and using fresh Hematoxylin each time. Being incubated in dH_2O for 45 seconds, slides were placed in HCl-ethanol solution for 15 seconds and then wash with dH2O for 15 seconds. Subsequently, slides were incubated in 1% lithium carbonate solution for 15 seconds, in dH2O for 15 seconds and in Eosin Y Alcoholic for 15 seconds. Slides were transferred to 95% ethanol for 15 seconds incubation repeating this step a 2^{nd} and 3^{rd} time using fresh 95% ethanol. Then slides were placed in in 100% ethanol for 15 seconds and were transferred to fresh 100% ethanol for 45 seconds incubation. After being incubated in xylene for 45 seconds and finally to air dry and coverslip the slide using mounting media, the stained slides were completed.

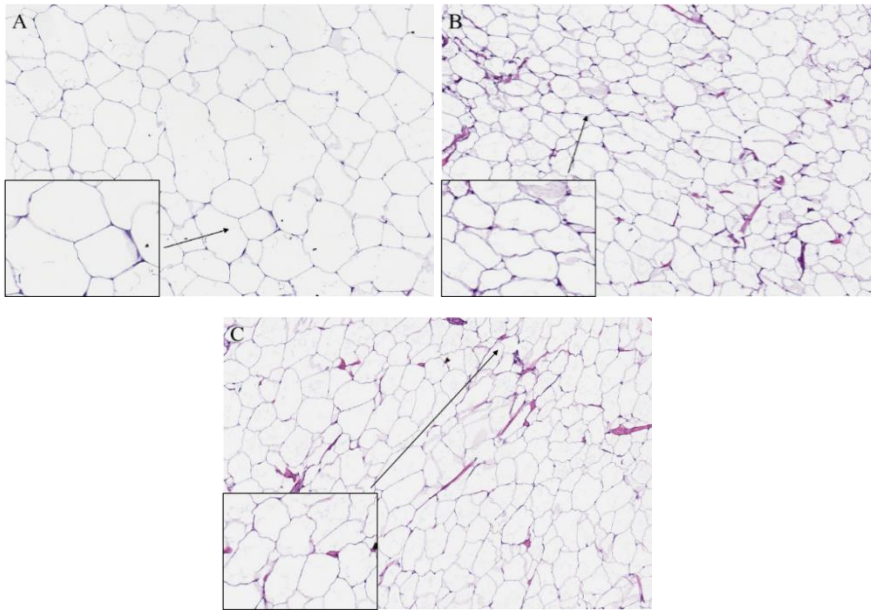

Fig. 13 *Imgages of H&E stained paraffin sectioned adipose tissues. (A=Visceral fat tissue, B= Belly flap and C=Dorsal fat layers)*

3.2.3.2 Image analysis

Ten slides of tissue section for three different fat tissues (Visceral fat tissue, Belly flap and Dorsal fat) were taken from February 2019 fish samplings. The histology sections were observed at 10X magnification opened in the software ImageScope. Three snapshots from the top, central and bottom region of each slide

were obtained (Fig. 14). Each snapshot is supposed to be filled with only adipocytes which are not broken cells, and there should neither be too much muscle tissues nor any blank area in the snapshot.

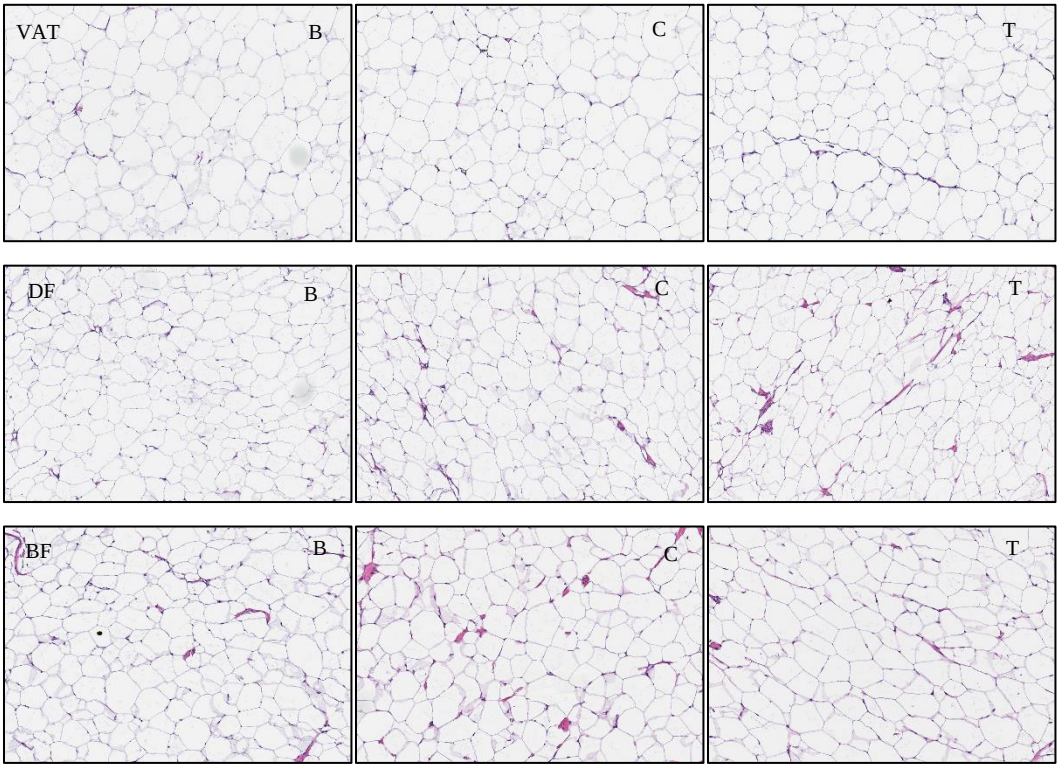

Fig. 14 *Microscopy images (X 20 magnification) obtained by ImageScope from three different fat tissues section (Visceral fat tissue (VAT), Belly flap (BF) and Dorsal fat (BF)) of Atlantic salmon. B (Bottom), C (Central) and T (Top) represent the area where the snapshot was taken.*

The measurements of cross-sectional areas of adipocytes were accomplished by using ImageJ software. Firstly, the scale of each snapshot was set up before processing, which was accomplished by using 'straight line' tool to draw one equal straight line of Scalebar which is in the bottom left corner of the snapshot. Then clicking 'set scale' under 'analyze', in this table, 'known distance' was filled with the distance of Scalebar, and the 'distance in pixel' was filled with the distance of the 'straight line' which was drawn before (Fig.15). The Scale was checked out when opening one new image in the program to ensure all the snapshots are under the same criterion.

For the measurements of adipocyte cell size and numbers, obtained images were needed to be processed first. The color type of each image was changed from RGB color to 8-bit. Then the brightness and contrast of the images were adjusted until that cell plates and some black dots inside cells were nearly invisible. Subsequently 'Threshold' command was used to erase the white dots inside cells even though some part of

membrane line was slightly disappeared. The last step was using 'Watershed' to get binary images. The binary images were compared with the original ones to ensure an accurate conversion. And Those 'fake' membrane lines were erased manually by using 'Paintbrush' tool.

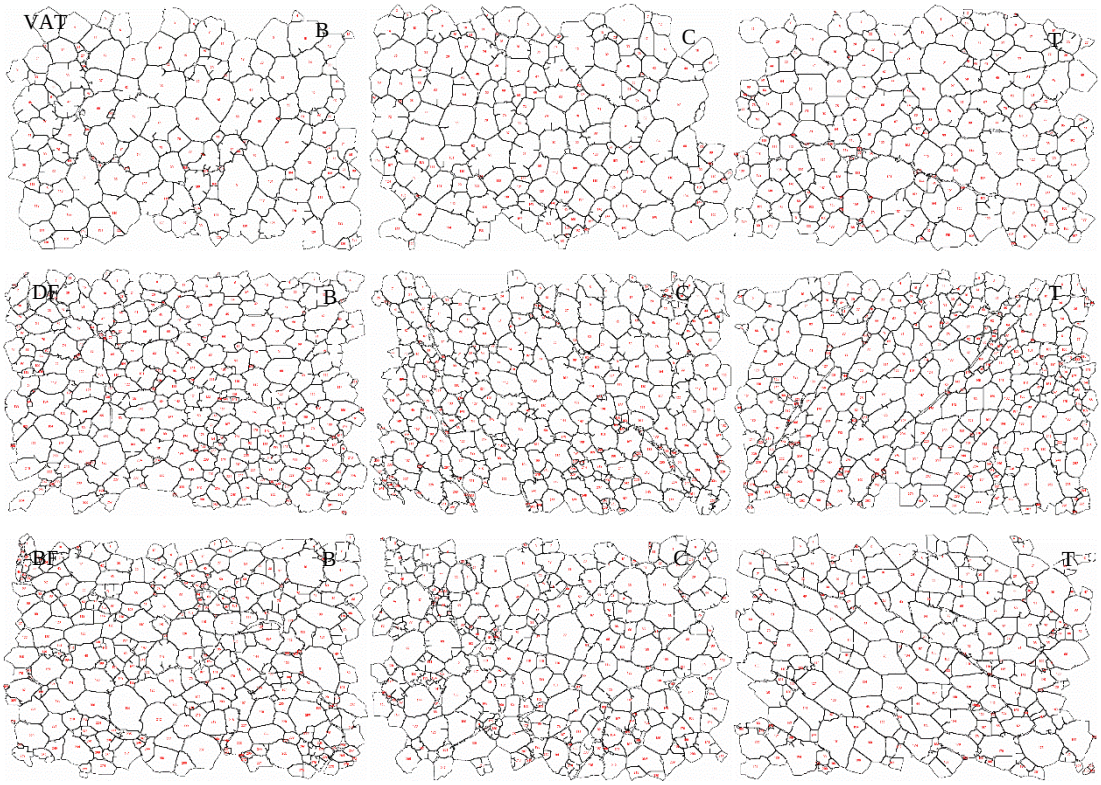

Fig. 15 *The same images obtained from ImageScope processed by ImgaeJ show the results of number and size of adipocytes (Visceral fat tissue (VAT), Belly flap (BF) and Dorsal fat (BF)) B (Bottom), C (Central) and T (Top) represent the area where the image was taken.*

Before starting analysis, under 'Set Measurements' table, only the 'Area' and 'shape descriptors' were presented in the results. And cells smaller than 50μm^2 were considered to represent artifacts from the image-conversion process and excluded. And the cells located on edge were excluded as well. Data of each snapshot of tissue sections was divided into four ranges: 50-300μm^2, 300-2500μm^2 ,2500-7000μm^2, and bigger than 7000μm^2. And the results were directly loaded into Excel for further analysis.

3.2.4 Microarray analysis

messenger RNA (mRNA) isolation

After Atlantic salmon were killed, around mg of the dorsal and visceral tissues were collected from each fish. The animal experiments were approved by the local ethical committee. For optimal results, harvested tissue is stabilized immediately in RNA*later* RNA Stabilization Reagent, then frozen in liquid nitrogen, and stored at -80°C. β-mercaptoethanol (β-ME) is added to Buffer RLT Plus before use (Add 10 µl β -ME per 1 ml Buffer RLT Plus). The weighed tissue is immediately placed in liquid nitrogen and be grinded thoroughly with a mortar and pestle. Then tissue powder and liquid nitrogen were transferred into an RNase-free, liquid-nitrogen–cooled, 2 ml microcentrifuge tube (Allow the liquid nitrogen to evaporate, but do not allow the tissue to thaw). 350 µl of Buffer RLT Plus is added, and the lysate is pipetted directly into a QIAshredder spin column placed in a 2 ml collection tube with 2 min centrifugation at maximum speed. The supernatant is carefully removed by pipetting and then lysate is transferred to a gDNA Eliminator spin column that is placed in a 2 ml collection tube. After 30s at 8000g centrifugation, the flow-through in the collection tube is saved. 350 µl of 70% ethanol is added to flow-through then mixed well by pipetting. Up to 700 µl of sample including any precipitate to a RNeasy spin column placed in a 2 ml collection tube of r 15s centrifugation at 8000g with flow-through discarded. Reusing collection tube, 700 µl Buffer RW1 is added to the RNeasy spin column that is then centrifuged for 15s at 8000g with flow-through discarded. The RNeasy spin column is carefully removed from the collection tube so that the column does not contact the flow-through. The flow-through is discarded again. 500 µl Buffer RPE is added to the RNeasy spin column for 15s centrifugation at 8000g, and the flow-through is discarded. 4 volumes (350 µl as one volume) of ethanol (96–100%) are added to Buffer RPE to obtain a working solution before use. Repeatedly, another 500 µl Buffer RPE is added to RNeasy spin column that is centrifuged for 2 min at 8000g. Subsequently, RNeasy spin column is transferred to a new 2 ml collection tube with the old collection tube discarded. The column with the tube is centrifuged full speed for 1 min. After being placed in a new 1.5 ml collection tube, RNeasy spin column is added with 50 µl RNase-free water. Steps of the procedure are quickly performed at room temperature, and all centrifugation steps are at 20–25ºC in a standard microcentrifuge.

Probe labeling and purification

RNA was treated with RNase-free DNase I, to remove any contaminating DNA. The total RNA concentration and quality were determined by spectrophotometry. And all RNA samples used in our experiments had A260/280 ratios between 1.80 and 2.30. Two to 4 µg mRNA were used from each group of animals for each experiment. Equal inputs from 8 individual replicates were pooled for individual dorsal or visceral adipose tissue microanalysis. Equalized control was made by mixing RNA obtained form

visceral or dorsal tissues from each individual fish. The test and control samples were labelled with respectively Cy5-dUTP and Cy3-dUTP. The fluorescent dyes were incorporated in cDNA using the SuperScript™ Indirect cDNA Labelling System. Labeled cDNA was produced by a random primed RT reaction in the presence of Cy-labeled nucleotides. The cDNA synthesis was performed at 46°C for 3 h in a 20 µl reaction volume, following RNA degradation with 0.2 M NaOH at 37°C for 15 min and alkaline neutralization with 0.6 M Hepes. Labelled cDNA was purified with Microcon YM30.

Solution hybridization

The slides were pretreated with 1%BSA fraction V, 5 × SSC, 0.1% SDS (30 min at 50°C) and washed with 2 × SSC (3min) and 0.2 × SSC (3min) and hybridized overnight at 60°C in a cocktail containing 1.3 × Denhardt's, 3 × SSC 0.3% SDS, 0.67 µg/µl polyadenylate and 1.4 µg/µl yeast tRNA. After hybridization slides were washed at room temperature in 0.5 × SSC and 0.1% SDS (15min), 0.5 × SSC and 0.01% SDS (15 min), and twice in 0.06 × SSC (2 and 1 min, respectively).

Image analysis

Scanning was performed with Axon GenePix 4100A and images were processed with GenePix 6.0. The spots were filtered by criterion (I-B)/(SI+SB) $\geqslant$ 0.6, where I and B are the mean signal and background intensities and SI, SB are the standard deviations. Low quality spots were excluded from analysis, and genes presented with less than three high quality spots on a slide were discarded. After subtraction of median background from median signal intensities, the expression ratios were calculated. Lowess normalization of $\log_2$-expression ratios was performed. The differential expression of selected genes was assessed by difference of the mean log-expression ratios between the slides with reverse labelling (5 spot replicates per gene on each slide, Student's t-test, $p < 0.01$).

4 Results

4.1 Fluorescence staining of adipocytes

This trial was conducted in order to study what are the difference on intracellular lipids content level numbers of cells between differentiated visceral and subcutaneous adipocytes. After reached the differentiated stage, at day 15, the cells were processed to conduct the staining experiment.

The differentiated adipocytes analysis by Lipid Tox staining:

The differentiated subcutaneous adipocytes were stained with the LipidTOX Green Stain and the lipid droplets signals were captured by the microscope Fig.16. We observed that the subcutaneous adipocytes are more fibroblast-like shape. According to the green signals, only few small lipid droplets were fusing with larger ones, and most lipid droplets were distributed widely inside the cells. Besides, it seems that there were more subcutaneous adipocytes than visceral adipocytes at the same magnification.

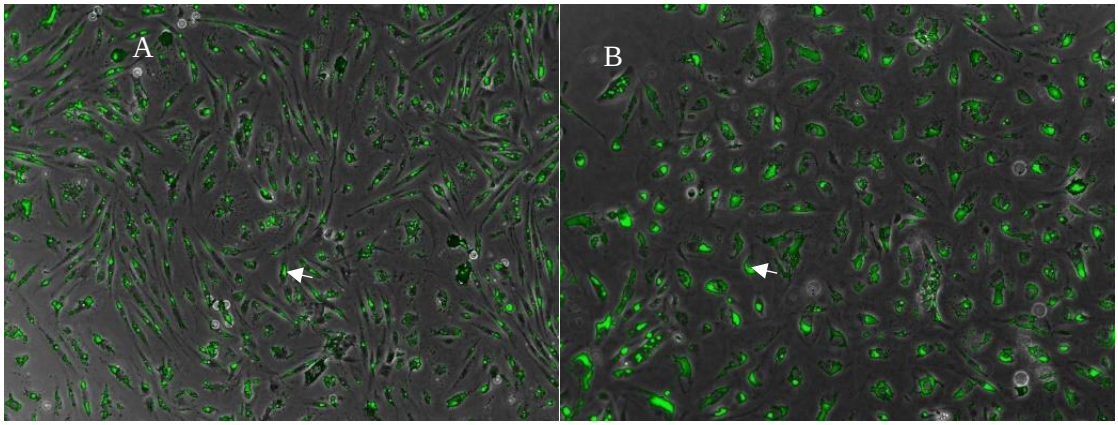

Fig. 16 *Micrograph shows Lipid Tox Stain in different Atlantic salmon adipocytes (Subcutaneous adipocytes (A) and visceral adipocytes (B)) in vitro cultivation at day 15; magnification 10X. Arrows=Lipid droplets(green).*

Compared to the subcutaneous adipocytes, the visceral adipocytes are more rounded in shape and bigger., which can also be found in ORO and Coomassie blue Stain. The more widespread and larger green signal in visceral adipocytes indicated that there were more intracellular lipid droplets.

The differentiated adipocytes analysis by oil red O(ORO) and Coomassie blue Stain:

This trial was conducted in order to quantify the intracellular lipid content level and cell density of two types of adipocytes. Then the proteins were stained with Coomassie blue stain, and microscopy images were taken after staining.

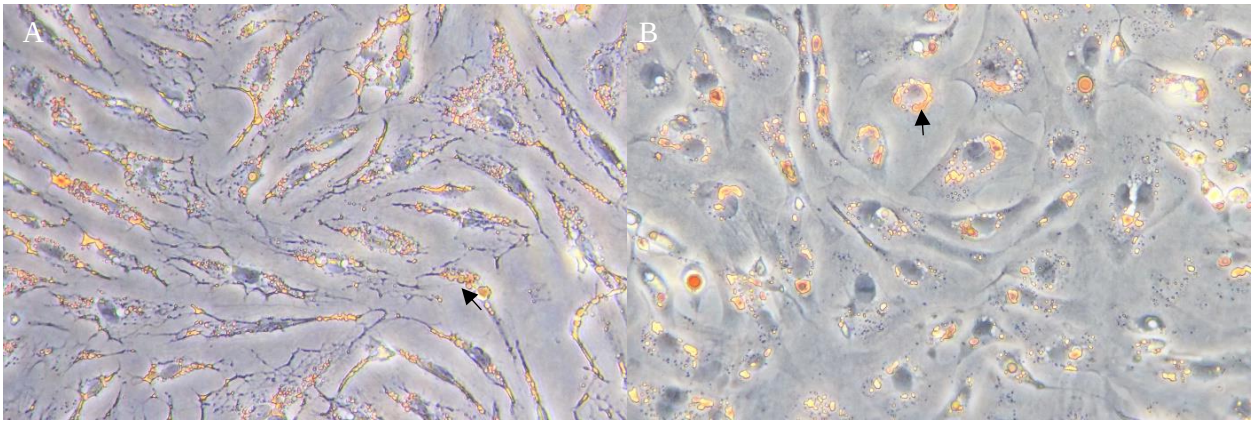

Fig. 17 *Micrograph shows oil Red O staining (ORO) in different Atlantic salmon adipocytes (Subcutaneous adipocytes (A) and visceral adipocytes (B)) in vitro cultivation at day 15, magnification10X. Arrows=Lipid droplets(orange).*

After staining, the lipids droplets showed bright orange color and protein with blue color (cell nucleus were more visible) Fig.18. Compared with Lipid Tox staining, the similar phenomenon was observed that there were more small widespread lipid droplets inside the subcutaneous adipocyte, while the intracellular lipid droplets of visceral adipocytes were bigger and were accumulated around cell nucleus.

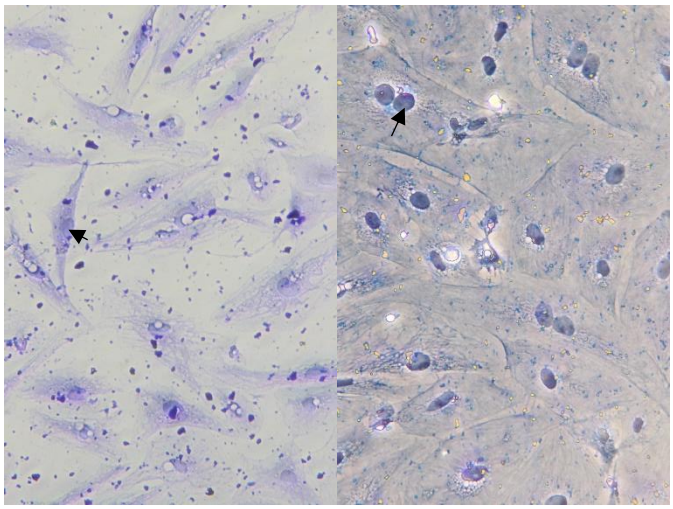

Fig. 18 *Micrograph shows oil Coomassie blue Stain in different Atlantic salmon adipocytes (Subcutaneous adipocytes (A) and visceral adipocytes (B)) in vitro cultivation at day 15, magnification10X. Arrows=nucleus.*

The proteins-stained images showed the nucleus and membrane of cells more clearly Fig.17. We observed that the visceral adipocytes were bigger than subcutaneous adipocytes in vitro cultivation. The fibroblastic cell shape of subcutaneous adipocytes and spherical cell shape visceral adipocytes have been confirmed.

To analyze the lipid content levels and cell density for two type cells, the quantification experiment was conducted. After images were captured, the protein and lipid levels are detected (6 well replicates for each type of adipocytes). The results showed that the intracellular lipid content levels were much higher in visceral adipocytes than that in subcutaneous adipocytes Fig.19. This may imply the stronger capacity of accumulating lipid in visceral adipocytes in comparison to subcutaneous adipocytes.

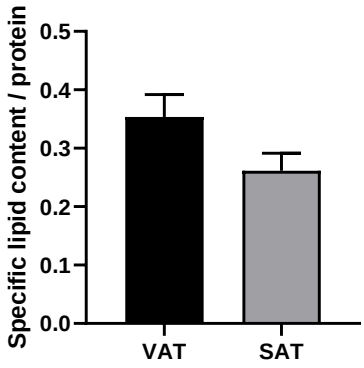

Fig. 19 *The intracellular lipid concentration analysis in two different types of differentiated adipocytes at day 15 (visceral adipocytes (VAT) and subcutaneous adipocytes (SAT)). Data are shown as mean ± SEM (n =6).*

4.2 The histological differences of adipocytes from different fat depots

The data of the cell population and cell size from three different fat tissues (Visceral fat tissue, Belly flap and Dorsal fat) has been processed to detect the histological differences among them, which is shown in Fig.20.The number of cells showed significantly differences between visceral adipose tissue and the other two fat tissues (belly flap and dorsal fat). Visceral fat tissue contained much less adipocytes, while the size of visceral adipocytes was much larger than the two other types of adipocytes (Fig.20). It is shown that the average size of visceral adipocyte is almost twice lager than that of subcutaneous adipocytes, while the average subcutaneous cell population is twice than visceral.

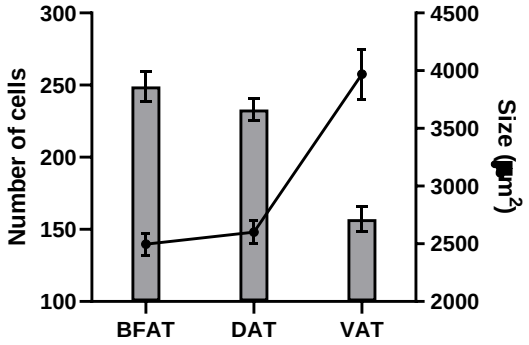

Fig. 20 *The histology analysis from three different tissues. The curve represents size distribution, and the bar represents the quantity distribution of cells. Data are shown as mean ± SEM (n = 10). (BF=Belly flap tissue, DF=Dorsal fat tissue and VAT=visceral fat tissue).*

It seems that belly flap and dorsal fat tissues represented quite similar result. They contain nearly the same amounts of adipocytes with similar cellular size. To get more detailed information in each fat depot the frequency distributions of adipocyte cell area from BFAT, DAT and VAT groups are shown in Fig.21. All adipocytes from both BFAT and DAT group showed their maximum relative frequency in the 300-2500μm^2 range, while the adipocytes form VAT accounts for the biggest proportion in 2500-7000μm^2 range. For those extremely large cells (7000-∞μm^2), VAT group shows a much higher relative frequency than the other two groups. It takes up almost 20% of all the cells in VAT group, while there are respectively less 10% of extremely large cells (7000-∞μm^2) in BFAT and DAT group.

In 50-300μm^2 range all the groups show the low frequency and VAT is lower than the two other groups. In the comparison between BFAT and DAT group, DAT group does not present a big frequency difference between 300-2500μm^2 and 2500-7000μm^2 range like BFAT group.

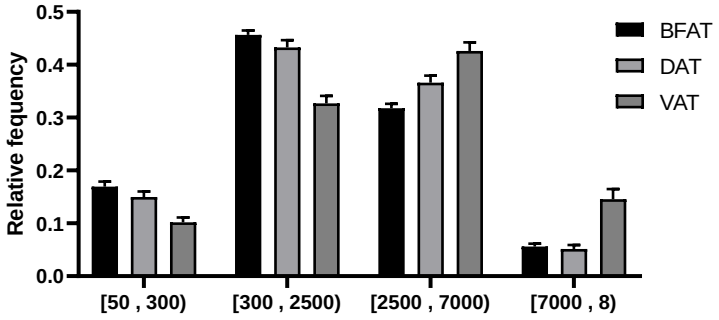

Fig. 21 *adipocyte cell size distribution analysis. Cells are classified into four scales according to size range. Data are shown as mean ± SEM (n = 10).*

4.3 Up-regulated genes in dorsal adipose tissue

The transcriptome profile from different adipose tissues is compared to identify the potential developmental and functional differences between them. A total of 1329 genes were differently expressed, which are main classified into four classes: cell structure, tissue structure and development, and immune.

4.3.1 Metabolism Calcium

The gene coding for transporter proteins like ATP2A1, SLC25, and S100A1 that transfer calcium is highly expressed in dorsal adipose tissue compared to visceral adipose tissue (Table 2). Sarcalumin is responsible for calcium buffering in the lumen of the sarcoplasmic reticulum and helps out calcium pump proteins. Parvalbumin beta 1 contributes to Ca^{2+} removal from the cytoplasm. And S100 calcium-binding protein A1 expressed in individual cells allows cells to transduce changes in calcium levels into unique biological responses. The expression of these genes related to metabolism calcium is highly induced in dorsal fat, which implies the high levels of calcium transportation occurring in this type of tissue.

Table 2 Results of microarray analyses, selected genes with expression changes. Samples from dorsal fat tissue (8 pooled fish individual per location) were compared to that from visceral fat tissue. Data are log-ER (expression ratios). Significantly up-regulated genes ($p < 0.01$, t-test, 5 spot replicates per gene) are highlighted with red scales.

Metabolism Calcium		
Gene	Symbol	Dorsal/Visceral
ATPase Ca^{2+} transporting cardiac muscle fast twitch 1	ATP2A1	**5.64**
Sarcalumenin	SAR	**3.84**
parvalbumin beta 1	PVALB1	**7.19**
Solute carrier family 25	SLC25	**2.55**
S100 calcium binding protein A1	S100A1	**1.73**
Calsequestrin 2	CASQ2	**1.06**

4.3.2 Tissue ECM collagen

Correspondingly, with the high concentration of Ca^{2+} in the extracellular matrix, up-regulation was shown by several genes involved in cell contacts and adhesion (Table 3). For instance, COL14A1 plays a role in collagen binding and cell-cell adhesion, which was highly expressed. And the type XV collagen and type

VII collagen were found in dorsal fat. COL15A1 that has the strongest expression in the basement may function to adhere basement membranes to underlying connective tissue stroma, and COL7A1 functions as an anchoring fibril between the external epithelia and the underlying stroma.

Similar transcription changes were displayed by genes encoding collagens of different types. The expression of COL2A1 is elevated in dorsal fat. It is responsible for the production of the pro-alpha1(II) chain of type II collagen, which adds structure and strength to connective tissues. It is found primarily in cartilage and the vitreous humor of the eye. Three pro-alpha1(II) chains twist together to form a triple-stranded, ropelike procollagen molecule. After being processed by enzymes in the cell, they leave the cell and cross-link themselves on another in the space around cells, which results in the formation of strong mature type II collagen fibers.

Similar up-regulation was also found in COL1A1, COL11A2, and COL16A1. Type XI and I collagens are found in most connective tissues, including cartilage, and they make a molecule of their procollagen like COL2A1. Additionally, it is shown that type XI collagen also helps maintain the spacing and diameter of type II collagen fibrils. Type XVI collagen is found in association with fibril-forming collagens such as type I and II and serves to maintain the integrity of the extracellular matrix.

Table 3 Results of microarray analyses, selected genes with expression changes. Samples from dorsal fat tissue (8 pooled fish individual per location) were compared to that from visceral fat tissue. Data are log-ER (expression ratios). Significantly up-regulated genes ($p < 0.01$, t-test, 5 spot replicates per gene) are highlighted with red scales.

Tissue ECM collagen		
Gene	Symbol	Dorsal/Visceral
Collagen alpha 1(XV) chain	COL15A1	**3.56**
Collagen alpha 1(XIV) chain	COL14A1	**2.92**
Alpha-1 type I collagen	COL1A1	**2.94**
Collagen, type II, alpha 1	COL2A1	**1.94**
Collagen alpha 2(XI) chain	COL11A2	**3.50**
Collagen alpha 1(XVI) chain	COL16A1	**1.53**
Alpha-1 type X collagen precursor		**1.64**
Collagen alpha 1(VII) chain	COL7A1	**2.35**

4.3.3 Tissue bone cartilage

The result of the high expression of cell contacts and adhesion gens and collagen genes was in accordance with the induced bone formation genes (Table 4). For example, POSTNB gene product, an osteoblast-specific protein with an important role in cell-collagen interactions, and matrilin-2-like, this family of proteins is thought to be involved in the formation of filamentous networks in the extracellular matrices of tissues, were highly expressed in the dorsal adipose tissue. This interaction of these genes suggested the potential development of tissue bone cartilage.

This up-regulation of the gene encoding the alpha chain of type X collagen precursor also verified this result since type X collagen was shown to be involved in the endochondral ossification of hypertrophic chondrocytes.

Table 4 Results of microarray analyses, selected genes with expression changes. Samples from dorsal fat tissue (8 pooled fish individual per location) were compared to that from visceral fat tissue. Data are log-ER (expression ratios). Significantly up-regulated genes ($p < 0.01$, t-test, 5 spot replicates per gene) are highlighted with red scales.

Tissue bone cartilage		
Gene	Symbol	Dorsal/Visceral
Periostin osteoblast specific factor b	POSTNB	**4.91**
Periostin osteoblast specific factor	POSTN	**1.09**
Cartilage acidic protein 2	CRTAC2	**1.66**
matrilin-2-like	MATN2	**2.42**

4.3.4 Sugar and energy metabolism

We observed the extremely high expression of a series of genes relating to the metabolic pathway of glycolysis and glycogen degradation (Table 5). Glycolysis is the metabolic pathway that converts glucose into pyruvate and a hydrogen ion. The free energy released in this process is used to form the high-energy molecules ATP (adenosine triphosphate) and NADH (reduced nicotinamide adenine dinucleotide).

GPI gene is highly induced in dorsal adipose tissue. Its gene products, glucose-6-phosphate isomerase, functions to interconvert glucose-6-phosphate (G6P) and fructose-6-phosphate (F6P) in the cytoplasm. 6-phosphofructokinase, muscle type is involved in the irreversible reaction that catalyzes the phosphorylation

of fructose-6-phosphate to fructose-1,6-bisphosphate, which serves as the major rate-limiting step of glycolysis. The expression of the gene encoding 6-phosphofructokinase was enhanced as well and mutations in this gene have been associated with glycogen storage disease type VII.

Table 5 Results of microarray analyses, selected genes with expression changes. Samples from dorsal fat tissue (8 pooled fish individual per location) were compared to that from visceral fat tissue. Data are log-ER (expression ratios). Significantly up-regulated genes ($p < 0.01$, t-test, 5 spot replicates per gene) are highlighted with red scales.

Sugar and energy metabolism		
Gene	Symbol	Dorsal/Visceral
Creatine kinase, muscle a	MCK	**3.63**
Glucose-6-phosphate isomerase	GPI	**4.43**
6-phosphofructokinase, muscle	PFKM	**4.48**
Fructose-bisphosphate aldolase	ALDO	**4.74**
Glycerol-3-phosphate dehydrogenase	GPDH	**3.39**
Triosephosphate isomerase	TPI1	**2.0**
Phosphoglycerate kinase	PGK	**0.98**
phosphoglycerate mutase 1 (brain)	PGAM1	**4.09**
Beta enolase	ENO3	**2.83**
Alpha enolase	ENO1	**1.77**
Pyruvate kinase, muscle, b	PKM2	**5.64**
Glycogen phosphorylase, brain	PYGB	**3.86**
Phosphoglucomutase 1	PGM1	**1.45**
Lactate dehydrogenase A	LDHA	**3.25**

The up-regulation was shown in the expression of the ALDO and TPI1 gene. The gene product of ALDO catalyzes a reversible reaction that splits the aldol, fructose 1,6-bisphosphate, into the triose phosphates dihydroxyacetone phosphate (DHAP) and glyceraldehyde 3-phosphate (G3P). Correspondingly, the expression of the TPI1 gene was enhanced. And its gene product triosephosphate isomerase encoded catalyzes the isomerization of G3P and DHAP in glycolysis and gluconeogenesis respectively.

Although the expression of PGK (Phosphoglycerate kinase), a major enzyme used in the first ATP-generating step of the glycolytic pathway was enhanced in dorsal fat tissue, there is much stronger induction (up to 6 folds) in the expression of PKM2 (Pyruvate kinase, muscle, b) that is the enzyme involved in the

last step of glycolysis. It catalyzes the transfer of a phosphate group from phosphoenolpyruvate (PEP) to adenosine diphosphate (ADP), yielding one molecule of pyruvate and one molecule of ATP.

The other genes involved in the glycolysis were upregulated as well in dorsal fat tissue such as PGAM1 (phosphoglycerate mutase 1 brain), ENO1 (Alpha enolase), and ENO3 (Beta enolase). Phosphoglycerate mutase 1 brain catalyzes the internal transfer of a phosphate group from C-3 to C-2 which results in the conversion of 3-phosphoglycerate (3PG) to 2-phosphoglycerate (2PG) through a 2,3-bisphosphoglycerate intermediate. As enolase, ENO3 and ENO1 are the glycolytic enzymes that catalyze the reversible conversion of 2-phosphoglycerate to phosphoenolpyruvate.

Interestingly, the expression of some genes that interact with the intermediates produced by glycolysis was increased as well. For instance, Glycerol-3-phosphate dehydrogenase (GPDH), an enzyme that catalyzes the reversible redox conversion of dihydroxyacetone phosphate to sn-glycerol 3-phosphate and serves as a major link between carbohydrate metabolism and lipid metabolism and contributes electrons to the electron transport chain in the mitochondria, was highly induced. Besides, Phosphoglucomutase 1 (PGM1) that catalyzes the bi-directional interconversion of G1P and glucose 6-phosphate G6P and lactate dehydrogenase A that catalyzes the inter-conversion of pyruvate and L-lactate with concomitant interconversion of NADH and NAD^+ were both shown to be more expressed in dorsal fat.

In glycogen degradation, glycogen phosphorylase brain (GPBB) catalyzes the phosphorolysis of glycogen to yield glucose 1-phosphate, which serves as the rate-determining first step in glycogenolysis. The expression of PYGB gene was highly enhanced.

Creatine kinase (CK), also known as creatine phosphokinase (CPK), is an enzyme that plays an important role in energy metabolism. CK catalyzes the reversible conversion of creatine and uses ATP to create phosphocreatine (PCr) and ADP. PCr serves as an energy reservoir for the rapid buffering and regeneration of ATP in situ, as well as for intracellular energy transport by the PCr shuttle or circuit. The result of the high expression of MCK gene was consistent with the markedly enhanced expression of those enzyme genes involved in glycolysis.

4.3.5 Tissue growth factor

We observed the up-regulation of a series of genes involved in cell proliferation, such as FGF12, Grb2, IGFBP7, and HTRA1(Table 6). It is shown that inhibition of Grb2 function impairs developmental processes in various organisms and blocks the transformation and proliferation of various cell types.

Table 6 Results of microarray analyses, selected genes with expression changes. Samples from dorsal fat tissue (8 pooled fish individual per location) were compared to that from visceral fat tissue. Data are log-ER (expression ratios). Significantly up-regulated genes ($p < 0.01$, t-test, 5 spot replicates per gene) are highlighted with red scales. Data are folds to

Tissue growth factor		
Gene	Symbol	Dorsal/Visceral
Fibroblast growth factor 12	FGF12	**2.13**
Follistatin-like 3 glycoprotein	FSTL3	**1.73**
Growth factor receptor-bound protein 2	GRB2	**3.39**
Insulin-like growth factor-binding protein 7	IGFBP7	**0.99**
Mimecan	OGN	**8.42**
Mimecan precursor		**3.31**
SPARC precursor		**1.04**
Transforming growth factor beta-3	TGFB3	**1.83**
Serine protease HTRA1	HTRA1	**2.59**

Besides, some of these genes are involved in the regulation of insulin-like growth factors (IGFs). For instance, Insulin-like growth factor-binding protein 7 helps to lengthen the half-life of circulating IGFs in all tissues and may act to enhance or attenuate IGF signaling depending on their physiological context. And serine protease HTRA1 is a secreted enzyme that is proposed to regulate the availability of IGFs by cleaving IGF-binding proteins. FSTL3 was demonstrated to interact with an extracellular protein (a disintegrin and metalloprotease 12) that has been implicated in insulin-like growth factor signaling. All the highly induced expression of these genes indicated a more active insulin-like growth factor signaling in dorsal fat tissue.

The markedly high expressions of OGN and the gene encoding its precursor were noticed. OGN encodes a protein (Mimecan) which induces ectopic bone formation in conjunction with transforming growth factor-beta (TGF β). The induced gene encoding SPARC (Secreted protein acidic and rich in cysteine) precursor was observed, which function similarly in regulating cell growth through interactions with the extracellular

matrix and cytokines. It is shown that lack of SPARC might lead to the aberrant assembly of ECM that in turn affects the localization and subsequent activation of TGF-β. Correspondingly, the expression gene TGFB3 was increased. TGF-β3 (transforming growth factor beta-3) is believed to regulate molecules involved in cellular adhesion and extracellular matrix formation during the process of palate development and the development of lungs in mammals.

4.4 Up-regulated genes in visceral adipose tissue (suppressed in dorsal fat)

4.4.1 Protein degradation

Compared with the genes that were enhanced in dorsal fat, highly induced genes related to protein degradation were observed in visceral fat tissue (Table 7).

Table 7 Results of microarray analyses, selected genes with expression changes. Samples from dorsal fat tissue (8 pooled fish individual per location) were compared to that from visceral fat tissue. Data are log-ER (expression ratios). Significantly down-regulated genes ($p < 0.01$, t-test, 5 spot replicates per gene) are highlighted with green scales.

Protease		
Gene	Symbol	Dorsal/Visceral
Elastase-1	ELA1	**-5.90**
Chymotrypsin B	CRTB	**-7.17**
Trypsin-1	PRSS1	**-7.59**
Trypsin-2	PRSS2	**-7.66**
Trypsin-3	PRSS2	**-6.36**
Carboxypeptidase A2	CPA2	**-7.10**
Carboxypeptidase B1	CPB1	**-8.06**
Dipeptidase 1	DPEP1	-2.12
Carboxyl ester lipase		-5.59
Matrix metalloproteinase-9	MMP9	-2.14
Collagenase 3	MMP13	-1.49
Matrix metalloproteinase 14	MMP14	-1.18
Alpha-1-microglobulin	A1M	-3.00

Chymotrypsin-like elastase family member 1 (CELA1) also known as elastase-1 (ELA1) is an enzyme that is encoded by the CELA1 gene. It is a subfamily of serine proteases that hydrolyze many proteins in addition to elastin. This enzyme can induce acute pancreatitis in the animal. The expression of ELA1 gene was extremely induced in visceral adipose tissue.

We also observed the up-regulation of genes encoding a series of proteases that interacts with each other, such as chymotrypsin, trypsin, and carboxypeptidases (CP). Trypsin is formed in the small intestine when its proenzyme form, the trypsinogen produced by the pancreas, is activated. Trypsin functions in cutting peptide chains mainly at the carboxyl side of the amino acids lysine or arginine, breaking down proteins into smaller peptides. Similarly, as a digestive enzyme component of pancreatic juice acting in the duodenum, chymotrypsin performs the breakdown of proteins and polypeptides. Carboxypeptidases and Dipeptidase 1 (DPEP1) may function with those various oligopeptides and dipeptides, many of which resulted from the digestion of dietary proteins by pepsin, trypsin, and chymotrypsin.

The various matrix metalloproteinases were shown in visceral fat tissue, such as MMP9, MMP13, and MMP14. Collectively, these enzymes are capable of degrading kinds of extracellular matrix proteins. Besides, the highly induced carboxyl ester lipase (CEL) was observed, which aids in the digestion of fats. It is a lipolytic enzyme capable of hydrolyzing cholesteryl esters, tri-, di-, and mono-acylglycerols, phospholipids, lysophospholipids, and ceramide.

Interestingly, the gene encoding alpha-1-microglobulin (A1M) was upregulated. A1M is a small globular protein and is distributed in blood plasma and extravascular tissues of all organs. It has been proposed in the role that continuously removes free radicals and oxidizing agents from the tissues, which therefore believed to protect cells and tissues against the damage that is induced by oxidative stress.

4.4.2 Acute phase of inflammation

The acute-phase reaction is in response to inflammation characteristically involves fever, acceleration of peripheral leukocytes, circulating neutrophils and their precursors. A series of genes involved in the acute phase of inflammation were upregulated in visceral fat, such as CRP, SAA1, and SAA5 (Table 8).

C-Reactive Protein (CRP) is an acute phase protein that is synthesized in the liver and is most commonly used as a marker for inflammation. Its concentration in plasm increases following elevated interleukin-6 secretion by macrophages and T cells. Serum amyloid A (SAA) proteins are the family of apolipoproteins as well, which is associated with high-density lipoprotein (HDL) in plasma. They are secreted during the acute phase of inflammation, function with the recruitment of immune cells to inflammatory sites.

Table 8 Results of microarray analyses, selected genes with expression changes. Samples from dorsal fat tissue (8 pooled fish individual per location) were compared to that from visceral fat tissue. Data are log-ER (expression ratios). Significantly down-regulated genes ($p < 0.01$, t-test, 5 spot replicates per gene) are highlighted with green scales.

Acute phase		
Gene	Symbol	Dorsal/Visceral
Serum amyloid A5	saa5	-2.19
Serum amyloid A	Saa1	-2.05
C-reactive protein	CRP	-3.59
C-reactive protein similar,	APOC1	**-3.59**

4.4.3 Immune effector molecules

The increased expression of genes encoding the effector molecules that are in response to the inflammation process was found in visceral adipose tissue Table 9. PRF1 encodes perforin-1 that is a pore-forming cytolytic protein found in the granules of cytotoxic T lymphocytes (CTLs) and natural killer cells (NK cells). It binds to the target cell's plasma membrane and oligomerizes in a $Ca2^{+}$ dependent manner to form pores on the target cell, which allows for the passive diffusion of a family of pro-apoptotic proteases, known as the granzymes, into the target cell.

Ribonuclease and defensins have been shown to contribute to innate host defense via direct bactericidal activity as well as to adaptive immunity through effector and regulatory functions which are expressed either constitutively or induced upon a challenge. Their expression was highly enhanced as well.

We observed some genes that encode lysozymes were upregulated such as lysozyme C II, lysozyme G-like and Myeloperoxidase (MPO). Lysozymes is an antimicrobial enzyme produced by animals, that forms part of the innate immune system. It functions in catalyzing the hydrolysis of 1,4-beta-linkages between N-acetylmuramic acid and N-acetyl-D-glucosamine residues in peptidoglycan, which is the major component of the gram-positive bacterial cell wall. This hydrolysis compromises the integrity of bacterial cell walls causing lysis of the bacteria. MPO is a peroxidase enzyme and a lysosomal protein that produces hypochlorous acid (HOCl) from hydrogen peroxide (H^2O^2) and chloride anion (Cl^{-}) and oxidizes tyrosine to the tyrosyl radical using hydrogen peroxide as an oxidizing agent, which are used by the neutrophil to kill bacteria and other pathogens. Some other proteins that have antimicrobial activity were also expressed in this type of fat like Neutrophil cytosol factor 1 and liver-expressed antimicrobial peptide 2.

Table 9 Results of microarray analyses, selected genes with expression changes. Samples from dorsal fat tissue (8 pooled fish individual per location) were compared to that from visceral fat tissue. Data are log-ER (expression ratios). Significantly down-regulated genes ($p < 0.01$, t-test, 5 spot replicates per gene) are highlighted with green scales.

Acute phase		
Gene	Symbol	Dorsal/Visceral
Perforin-1	PRF1	-5.44
Ribonuclease-like 3	RNASEL3	-5.23
Defensin beta 3	DEFB3	-3.82
Myeloperoxidase (mpo)	MPO	-2.56
Neutrophil cytosolic factor 1	NCF1	-2.38
Liver-expressed antimicrobial peptide 2	LEAP2	-1.98
lysozyme C II		-2.17
lysozyme G-like	LYG1	-1.09

4.4.4 Immune T cell

It seems that visceral adipose tissue expressed different genes relating to the activation and regulation of T cells (Table 10). The up-expression of T-cell receptor (TCR) was found. TCR is a protein complex found on the surface of T lymphocytes (T cells), which is responsible for recognizing fragments of antigen as peptides that are bound to major histocompatibility complex (MHC) molecules. When the TCR engages with antigenic peptide and MHC (peptide/MHC), the T lymphocyte is activated through signal transduction. Upon binding to MHC, the TCR initiates a signaling cascade that is involved in transcription factor activation and cytoskeletal remodeling resulting in T cell activation. Besides, we observed the CD28 T-cell-specific surface glycoprotein high expression in visceral fat. CD28 (Cluster of Differentiation 28), known as one of the proteins expressed on T cells, provides co-stimulatory signals for T cells, which is required for T cell activation and survival. It has been suggested that T cell stimulation through CD28 in addition to the T-cell receptor (TCR) can provide a potent signal for the production of various interleukins (IL-6 in particular).

Table 10 Results of microarray analyses, selected genes with expression changes. Samples from dorsal fat tissue (8 pooled fish individual per location) were compared to that from visceral fat tissue. Data are log-ER (expression ratios). Significantly down-regulated genes ($p < 0.01$, t-test, 5 spot replicates per gene) are highlighted with green scales.

Acute phase		
Gene	Symbol	Dorsal/Visceral
Drebrin-like protein	DBNL	-1.48
CD28 T-cell-specific surface glycoprotein		-1.44
T-cell receptor		-1.07
CD3gammadelta-B		-1.27
CD3zeta-1		-0.98
Plastin-2 lymphocyte cytosolic protein	LCP1	-0.92
SH2 domain-containing protein		-0.88

Accordingly, some genes that are associated with signal transduction were induced as well, such as CD3gammadelta-B and CD3zeta-1gene. Their gene products CD3 (cluster of differentiation 3) is a protein complex and T cell co-receptor that is involved in activating both the cytotoxic T cell (CD8+ naive T cells) and T helper cells ($CD4^+$ naive T cells). It consists of a CD3γ chain, a CD3δ chain, and two CD3ε chains in mammals. These chains associate with the TCR and the ζ-chain (zeta-chain) to generate an activation signal in T lymphocytes.

The intracellular tails of the CD3γ, CD3ε, and CD3δ molecules each contain a single conserved motif known as an immunoreceptor tyrosine-based activation motif (ITAM), which is essential for the signaling capacity of the TCR. The intracellular tail of CD3ζ contains 3 ITAM motifs. These ITAMs can act as the binding site for SH2-domains of additionally recruited proteins through phosphorylation. Thus, it was not surprising that the SH2 domain-containing protein was highly expressed.

We also observed that several genes that may play a role in the activation of T-cells. It was suggested that Drebrin-like protein was involved in regulating T-cell activation by bridging TCRs and the actin cytoskeleton to gene activation and endocytic processes. And Plastin-2 lymphocyte cytosolic protein is involved in T cell activation by the co-stimulation through TCR/CD3 and CD2 or CD28.

4.5 Gens that were differently expressed

4.5.1 Lipid metabolism

We observed some genes belongs to the same function class were differentially expressed according to their location (Table 11). Although there was no significant difference between some transport proteins like CD36 antigen and Scavenger receptor class B member 1 in two types of fat tissues, the expression of fatty acid binding proteins that functions in intracellular FAs transportation was quite different. For instance, FABP10a was extremely induced in visceral fat, while FABP 4, FABP 7, and FABPH were highly elevated in dorsal fat. This suggested that those organ-specific fatty acid binding proteins were expressed differently according to the type of adipose tissue.

As mentioned early, the capability of β-oxidation of adipocyte in Atlantic salmon has been validated. However, by comparing the expression of CPT1B and CPT2 that are involved in the pathway fatty acid β -oxidation between dorsal and in visceral fat tissues, no significant differences were detected.

Remarkably, we observed a series of Apolipoprotein genes that were upregulated in dorsal adipose tissue. Apolipoprotein A1 is the major protein component of HDL particles, which enables efflux of fat molecules by accepting fats from within cells for transport (in the water outside cells) elsewhere, including back to LDL particles or the liver for excretion. In contrast, Apolipoprotein B-100 is one main isoform of apolipoprotein B. Apolipoprotein B, as a ligand for LDL receptors in various cells, mainly interacts with LDL, which is responsible for carrying fat molecules (lipids), including cholesterol, to all cells with ApoB receptors. Apolipoprotein C-I plays an important role in the exchange of esterified cholesterol between lipoproteins and in the removal of cholesterol from tissues. The up-regulation of these gene productions indicated the high levels of lipids transportation in visceral fat.

Table 11 Results of microarray analyses, selected genes with expression changes. Samples from dorsal fat tissue (8 pooled fish individual per location) were compared to that from visceral fat tissue. Data are log-ER (expression ratios). Significantly up-regulation and down-regulated genes ($p < 0.01$, t-test, 5 spot replicates per gene) are highlighted with red and green scales.

Lipid metabolism		
Gene	Symbol	Dorsal/Visceral
Fatty acid binding protein 10a, liver basic	FABP10A	-5.23
apolipoprotein A-I	APOA1	-1.28
Apolipoprotein C-I	APOC1	-2.60
Apolipoprotein CII	APOC2	-1.61
Apolipoprotein C-I precursor		-2.96
Apolipoprotein B-100	APOB	-2.33
Apolipoprotein-L3	APOL3	-1.01
Acetyl-CoA acetyltransferase, cytosolic	ACAT2	-0.85
Fatty acid-binding protein, adipocyte	FABP4	2.73
fatty acid-binding protein, brain	FABP7	1.75
fatty acid-binding protein, heart-like	FABPH	0.95
CD36 antigen	CD36	NS
Scavenger receptor class B member 1	SCARB1	NS
acyl-CoA-binding protein-like	ACBP	1.62
Adiponectin	ADIPOQ	2.40
leptin		NS
Carnitine palmitoyltransferase 1B (Muscle) - Ident 97	CPT1B	NS
CarnitineO-palmitoyltransferase 2, mitochondrial	CPT2	NS

4.5.2 Immune TNF

We did not find a significant expression difference of tumor necrosis factor alpha between visceral and dorsal adipose tissue (Table 12). However, genes expressed in dorsal and visceral fat were differentially regulated. Some genes were upregulated in visceral fat, such TSG6, TNFRSF10C, and DcR3, which both play protection mechanisms for cells. For instance, tumor necrosis factor-inducible gene 6 protein has recently been shown to protect the liver from acute damage. The gene product of TNFRSF10C is a receptor that has been thought to function as an antagonistic receptor that protects cells from TRAIL-induced

apoptosis. And the DcR3 receptor acts as a decoy receptor for TNF cytokine members, which inhibits the ability of the cytokines to signal for cell death or apoptosis.

In contrast, the high expression of RIPK1 and TIFA was shown in dorsal fat tissue. Receptor-interacting protein 1 and TRAF2-binding protein have been indicated to involve in cell death, which participates in the formation of TNFR-1 complex-I. It is formed firstly with the assembly of the TNF (tumor necrosis factor) ligand to its membrane receptor, the TNFR (tumor necrosis factor receptor). Once activated, the intracellular domain of TNFR starts the recruitment of the adaptor TNFR-1-associated death domain protein TRADD, which recruits RIPK1 and two ubiquitin ligases: TRAF2 and clAP1. The formed complex is called the TNFR-1 complex I. These results suggest dorsal fat tissue played a role in cell death with the association between TNFs.

Table 12 Results of microarray analyses, selected genes with expression changes. Samples from dorsal fat tissue (8 pooled fish individual per location) were compared to that from visceral fat tissue. Data are log-ER (expression ratios). Significantly up-regulation and down-regulated genes ($p < 0.01$, t-test, 5 spot replicates per gene) are highlighted with red and green scales.

Immune TNF		
Gene	Symbol	Dorsal/Visceral
tumor necrosis factor alpha		NS
Tumor necrosis factor-inducible gene 6 protein	TSG6	-2.79
tumor necrosis factor receptor superfamily member 10C-like	TNFRSF10C	-1.98
TNF decoy receptor	DcR3	-1.20
TNF alpha-induced protein 2, tnfaip2	TNFAIP2	-0.94
TRAF2-binding protein	TIFA	0.87
Receptor-interacting protein 1	RIPK1	2.01
TNF receptor-associated factor 4	TRAF4	1.04

4.5.3 Complement system

We observe a group of genes that are closely associated with complement system were highly induced in visceral fat tissue (Table 13). The high upregulation of C1q like protein, C2-like and C4-like indicated that the classical pathway occurring in the visceral fat tissue. We also found the induced C3 protein and its co-

effector complement factor D and B that was upregulated as well. These proteins paly an essential role in the alternative pathway of complement system. The expression of complement factor H and I also validated the presence of C3b that is generated from C3 by a C3 convertase enzyme complex and is also a crucial component of C3 convertase enzyme complex since complement factor H and I are involved in the inactivation of C3b. The up

The upregulation of these protein indicated the exist of both classical and alternative pathway in visceral adipose tissue.

Table 13 Results of microarray analyses, selected genes with expression changes. Samples from dorsal fat tissue (8 pooled fish individual per location) were compared to that from visceral fat tissue. Data are log-ER (expression ratios). Significantly up-regulation and down-regulated genes ($p < 0.01$, t-test, 5 spot replicates per gene) are highlighted with red and green scales.

Complement system		
Gene	Symbol	Dorsal/Visceral
complement component 1, q subcomponent-like 2	C1QL2	-3.32
Complement C1q-like protein 4 precursor		-2.77
Lectin (leca)		-1.96
Mannose receptor		-0.92
complement C3-like		-1.64
Complement C3		-1.45
Complement factor D precursor		-2.10
Complement factor Bf-1		-1.96
Complement factor I light chain	CFI	-1.41
complement factor H precursor	CFHL3	-2.37
complement factor H-like		-1.33
complement C2-like		-1.22
complement receptor type 2-like		1.18
complement C4-like		-0.85
complement component C6	C6	-2.34
complement component C7-like		-1.39
Complement component C8 beta	C8B	-2.50
Complement component 9, Perforin-1 precursor		-1.10

Complement factor D cleaves complement factor B into Ba and Bb interacting with C3b to form C3 convertase enzyme complex. In classical pathway, the C3 convertase enzyme complex is formed with

assembling C3b, C2a and C4b that are cleaved from C2 and C4 respectively. These C3 convertase enzyme complex also function in cleaving C5 to C5a and C5b that then recruits and assembles C6, C7, C8 and multiple C9 molecules to assemble the membrane attack complex. The expression of those Complement component C6, C7, C8, C9 relative genes suggested the formation of the membrane attack complex and validated the role of visceral adipose tissue in innate immune system (complement system).

Interestingly, we found the up-regulation of complement receptor type 2-like protein that binds to iC3b (inactive derivative of C3b) in dorsal fat tissue. The high presence of complement receptor type 2-like protein may indicate the deficiency in complement system in dorsal fat tissue since C3b were mainly proteolyzed into iC3b fragment.

5 Discussion

5.1 The morphology difference between different adipose tissue depots

Morphology is a significant characteristic when we study the various adipose tissue depots, which is defined as the number and size distribution of adipocytes within adipose tissue. Since adipose tissue is quite homogenous tissue, cell morphology in adipose tissue presents quite a difference compared with other tissue like skin in terms of different structures. Adipose tissue with fewer but larger adipocytes is said to have a 'hypertrophic' morphology, while adipose with many adipocytes of a smaller size is said to have a 'hyperplastic' morphology (Tandon et al., 2018). It has been shown that adipose morphology is in part determined genetically. Therefore, studying the morphology difference between various adipose tissue may help us predict their transcriptome difference and functional role. In our study, we mainly focus on the number and size distribution of adipocytes that belong to visceral fat tissue (VAT) and subcutaneous adipose tissue (SAT) of Atlantic salmon. We include both belly flap fat tissue and dorsal fat tissue divided into subcutaneous when they were compared with SAT, as they present a similar morphology result in histological analysis and are both located beneath the skin.

Fat cell size is a fundamental parameter in the study of adipose tissue metabolism since it markedly influences the cellular rates of metabolism. Our study showed that the VAT present 'hypertrophic' morphology, while SAT (in dorsal and ventral locations) had a 'hyperplastic' morphology. The average cell size of visceral adipocytes was significantly larger than subcutaneous adipocytes, while the average cell number present the opposite situation. This morphology difference is closely related to the main function of the visceral adipose tissue, which serves as the dominant lipids storage site that recruits much more lipids compared with subcutaneous adipose tissue.

Such a stronger ability of visceral adipocytes to accumulate intracellular lipids was then verified by observing the mature differentiated adipocytes morphology in vitro. By microscopy study, we captured stronger lipids signal in VAT compared with SAT. Although there have been few studies on lipid storage patterns in salmon muscle fibers and myosepta (Zhol et al., 1995; Zhou et al., 1996), establishing the knowledge about intracellular lipid storage is also crucial. In our study, both microscopy and fluorescence studies were used in vitro to evaluate the lipid content in both mature visceral and subcutaneous differentiated adipocytes. By microscopy study, we captured stronger lipids signal in visceral adipocytes compared with subcutaneous adipocytes, which suggested the intracellular lipid content in visceral adipocytes was significantly higher than that in subcutaneous adipocytes. A similar result was found in the

lipid class comparison in another study, which showed that visceral fat had significantly higher levels of lipid than belly flap (subcutaneous) of Atlantic salmon (Nanton et al., 2007). The higher intracellular lipid concentration in visceral adipocytes could be explained by the higher levels of some gene expression that these genes are closely related to FFAs uptake and lipid binding in VAT, such as the expression of fatty acid binding protein and apolipoprotein genes. The result from our microarray study in Atlantic salmon also showed the highly induced gene expression of the apolipoprotein family in visceral fat. According to our microarray result, apolipoprotein A1 and apolipoprotein B-100 were highly expressed in visceral fat, which interacts with HDL and LDL respectively. Apolipoprotein A1 enables the efflux of fat molecules by accepting fats from within cells, while apolipoprotein B-100 is responsible for carrying fat molecules (lipids), including cholesterol, to all cells with ApoB receptors. The gene transcriptome profile related to the apolipoprotein family indicated the capability of visceral fat tissue to store more lipids droplets inside cells.

As another morphology characteristic, the numbers of adipocytes in each visceral and subcutaneous adipose tissue have also been studied. In histology analysis, subcutaneous adipose fat (ventral and dorsal) contained a much greater number of adipocytes compared with visceral adipose fat. This finding may be explained by our microarray result, in which some tissue growth factor genes are upregulated such as FGF12, Grb2, IGFBP7. It has been suggested that the inhibition of Grb2 function impairs the transformation and proliferation of cells.

The result of the size distribution for belly flap and dorsal fat tissue showed that these two types of adipocytes were mostly distributed in 300-2500μm^2 range accounting for about 45% relative frequency. In contrast, the visceral adipose tissue with the 2500-7000μm^2 range has the biggest proportion. Two subcutaneous adipose tissue tends to produce more small cells (smaller than 300μm^2) than those extremely large cells (larger than 7000μm^2) in comparison to visceral adipose tissue processing more some extremely large cells than some small cells.

Such an adipocyte size distribution causes a smaller average size of subcutaneous adipocytes (around 2600 μm^2) than visceral adipocytes (around 4000μm^2). The smaller adipocytes in subcutaneous adipose tissue might significantly contribute to the maintenance of an energy supply since they have relatively more mitochondria associated with the main lipid body. This assumption is confirmed by the upregulation of a variety of energy metabolic enzyme genes showed by microarray results. However, the bigger size of adipocytes in visceral adipose tissue may be related to higher FFA mobilization and lipids accumulation in visceral fat.

5.2 Energy metabolism in subcutaneous adipose tissue

We observed the significant downregulation of adiponectin gene expression in VAT compared to SAT. tissue. The presence of adiponectin has been suggested to be accompanied by a reduction in plasma glucose an increase in insulin sensitivity in humans (Díez & Iglesias, 2003). This result is also in accordance with the finding that significant upregulation of leptin and downregulation of adiponectin gene expression has been found in mesenteric VAT compared to SAT in diabetic human obese individuals (Yang et al., 2008). Such downregulation of adiponectin gene expression suggested that VAT has higher levels of plasma glucose concentration, which maybe is the opposite in SAT. The upregulated expression of metabolic enzyme genes involved in glycolysis in SAT demonstrates this assumption.

From the microarray result, some genes that have been implicated in energy regeneration were higher expressed in SAT like PKM2, LDHA, and MCK, which suggested high free energy released from SAT in the form of ATP and DATH. The expression of PKM2 (Pyruvate kinase, muscle, b) was upregulated which is the enzyme involved in the last step of glycolysis yielding one molecule of pyruvate and one molecule of ATP. And LDHA gene product lactate dehydrogenase A catalyzes the inter-conversion of pyruvate and L-lactate with concomitant interconversion of NADH and NAD^+. MCK gene expresses creatine kinase that catalyzes the reversible conversion of creatine and uses ATP to create phosphocreatine (PCr) and ADP.

The higher levels of these metabolic enzyme genes indicate the powerful ability of SAT as a direct energy supply site compared with VAT providing the FFAs that are transported to other organs for oxidation.

5.3 Insulin association with visceral and subcutaneous adipose tissue

As we mentioned before, the presence of adiponectin has been suggested to be accompanied by an increase in insulin sensitivity. The higher expression of adiponectin in SAT compared with VAT may indicate that there an increase in the insulin resistance of VAT. This is proved by the upregulation of genes that are involved in the regulation of insulin-like growth factors in our microarray result, which indicated a more active insulin signaling pathway occurring in SAT than VAT.

In contrast, VAT seems is more related to insulin resistance. It has been suggested that insulin resistance is associated with an increase in CRP and SAA, which are both higher expressed in VAT than SAT. Besides, the proinflammatory amino-terminal kinase (JNK) pathway has been shown to interfere with insulin activity (Davis et al., 2000) and are activated by inflammatory cytokines and free fatty acids that are implicated in

the development of type 2 diabetes (Boden, 1997). Mice with a chromosomal deletion of JNK1 reduced adiposity, improved insulin sensitivity and enhanced insulin receptor signaling (Hirosumi et al., 2002). A higher amount of FFAs in VAT compared to SAT was found in our study may indicate the higher JNK activity in VAT causing higher insulin resistance of VAT.

Except these findings proving the insulin resistance of VAT, the higher expression of genes related to T cell activation and regulation in VAT compared to SAT suggests the high insulin resistance in VAT since some studies suggested that the inflammation in adipose tissue has been implicated in insulin resistance. (Nishimura et al., 2009) showed that the depletion of $CD8^+$ T cells weakens insulin resistance in obese mice, while adoptive transfer of $CD8^+$ T cells aggravated insulin resistance in obese mice. $CD4^+$ cells have a similar contribution to obesity-related insulin resistance, which was demonstrated by that impairing major histocompatibility complex (MHC) class II molecule (MHCII) on adipocytes is associated with improved insulin resistance in obese mice (Deng et al., 2013).

From the microarray result, we observed the higher expression of genes producing the protein complex that is involved in activating both $CD8^+$ and $CD4^+$ T cells in VAT compared with SAT. By combining these findings, we summarize that VAT has a higher insulin resistance compared to SAT being more insulin sensitive.

5.4 Lipid metabolism in visceral and subcutaneous adipose tissue

According to our microarray study, we found out the different gene expressions related to the lipid metabolism in SAT and VAT. Those genes have been shown to be implicated in the lipolytic and lipogenic activity of adipose tissue.

We observe there was a higher expression of a group of transporter proteins like ATP2A1, SLC25, and S100A in SAT than VAT. They play the role in transferring calcium, thus, regulating the intracellular calcium concentration. The upregulation of these genes indicates the existence of higher intracellular Ca2+ content in SAT compared with VAT. Some study has suggested the close relationship between intracellular Ca^{2+} and lipid metabolism in adipocytes. They demonstrated that the increasing adipocyte intracellular Ca^{2+} results in a coordinated stimulation of lipogenic gene expression and lipogenesis, and suppression of lipolysis, which causes lipid filling and increased adiposity in both human and mouse adipocytes (Zemel, 2003). It was showed in transgenic mice that increases dietary Ca^{2+} results in decreased intracellular Ca^{2+}, which exerted inhibition of adipocyte fatty acid synthase expression and stimulation of lipolysis (Zemel et al., 2000).

As we summarized in the last section, VAT has a higher insulin resistance compared to SAT being more insulin sensitive, such a mechanism is not only associated with the suppressed lipolysis activity in SAT but also higher lipolytic activity in VAT. It shows that the higher lipolytic activity in VAT in comparison to the SAT can also be attributed to the lipolysis-regulating hormones insulin that the antilipolytic effect of insulin is weaker in visceral than in subcutaneous adipose tissue (Björntorp, 1991). This presumption was verified by the enhanced expression of various genes that are involved in the regulation of insulin-like growth factors, which indicated a more active insulin signaling pathway occurring in SAT. For instance, the expression of IGFBP7 that helps to lengthen the half-life of circulating IGFs and HTRA1 that is proposed to regulate the availability of IGFs by cleaving IGF-binding proteins were upregulated in SAT.

The higher lipolytic activity may also result in more rapid mobilization of FFAs from visceral than from subcutaneous fat cells. This is also showed in both nonobese and obese human individuals, particularly in the latter, whose visceral fat cells have the stronger capability to mobilize FFAs compared with subcutaneous adipocytes (Wajchenberg, 2000). This phenomenon is consistent with the microarray result that the levels of FABP in visceral fat were higher than that in dorsal fat. An interesting finding was that different fatty acid binding proteins (FABP) isoforms were present in VAT and SAT. For instance, the liver FABP was more expressed in visceral fat, while brain, heart, adipocyte FABP were highly expressed in dorsal fat. Such tailoring of FABP expression profile was also found in issue-resident lymphocytes (Frizzell et al., 2020). This may imply that VAT in Atlantic salmon has a closer relationship with the liver in terms of lipids regulation compared with SAT.

Through all these findings, we conclude that VAT is more metabolically active to lipolysis, while SAT prone to inhibit lipolysis. This result is in accordance with the transcriptome characteristic of adipose tissue that VAT has the stronger ability to mobilize FFA and less to the anti-lipolytic action of insulin in comparison to SAT. The conclusion is consistent with the findings from human adipose tissue that the rate of lipolysis is low in the subcutaneous femoral/gluteal region high in the visceral (i.e. omental) region (Arner, 1995).

5.5 The immunity of visceral adipose tissue

Today, through the secretion of numerous adipokines, adipose tissue is considered to be an active endocrine and secretory organ with multiple functions in metabolic processes. The function role in the immunity of visceral adipose tissue is discussed in this section. According to our microarray result, it has been suggested that the visceral fat tissue paly an essential in both innate and adaptive immune system.

Acute phase proteins (APP's) are proteins whose serum concentrations either rise or fall in response to inflammation, which sometimes is referred to as the acute-phase response and this response is considered as the part of the innate immune system. We observe the higher expression of some acute phase proteins in VAT compared with SAT, such as C-Reactive Protein (CRP) and Serum amyloid A (SAA). The result is in accordance with the study that many of these additional factors including IL-6, α1 acid glycoprotein, and serum amyloid A (SAA) are expressed in adipose tissue of mice (Lin et al., 2001).

C-reactive protein (CRP) is an unspecific acute phase reactant serving as an excellent indicator of systemic inflammation (Pickup et al., 1997). The expression of these inflammatory markers in visceral adipose tissue proves the proinflammatory potential of visceral fat and also suggests the close relationship between visceral adipocytes and macrophages.

As part of the innate immune system, complement cascade functions by identifying bacteria, activating cells, and promoting clearance of antibody complexes or dead cells. The upregulation of complement factor genes indicates the function role of visceral fat that is involved in the complement system. All three different pathways (classical, alternative, and lectin pathways) were proved to be present in the visceral adipose tissue. It has been shown that the complement system triggers three different immune functions according to the three signaling pathways: Membrane attack-by rupturing cell wall of bacteria. (Classical Complement Pathway); phagocytosis-by opsonizing antigens through C3b (Alternative Complement Pathway) and inflammation- by attracting macrophages and neutrophils (Lectin pathway) (Murphy et al., 2017).

Additionally, it was found that the upregulated complement proteins in the adipocytes of non-obese human subjects are associated with familial combined hyperlipidemia, thus, suggesting the close relationship between increased complement gene expression and adipocyte insulin resistance and TG levels (van Greevenbroek et al., 2012). This may be explained by the high plasma ASP (also known as C3desArg that is a triplet produced C3, factor B, and factor D) that are often accompanied by enhanced AT expression of C3, factor B, and factor D. It was demonstrated that ASP has been shown to inhibit both basal and norepinephrine-triggered release of FFA by stimulating fractional FFA re-esterification (Van Harmelen et al., 1999) and promote TG synthesis by inducing diacylglycerol acyltransferase activity (Cianflone et al., 2004). Besides the VAT participates in the complement system, we also found the higher expression of some immune effector genes in VAT in comparison to SAT, that their gene products may contribute to the part function of the innate system, such as ribonuclease, defensins, lysozymes, and Myeloperoxidase.

It was found VAT is more actively participates not only in the innate immune system but also in the adaptive immune system by regulating T cells compared to SAT. According to our microarray result, the series of genes that are involved in the activation of T cells were higher expressed in VAT compared to SAT. For instance, T-cell receptor (TCR), CD3 (cluster of differentiation 3), CD28 (Cluster of Differentiation 28), and drebrin-like protein, that may directly participate in the signal transduction during the activation of T cell, indicating that VAT mainly plays an essential role in activating T cell in comparison with SAT. However, we found that the expression level of the adaptive genes was not strong as that of the genes involved in the innate immune system, which suggests VAT may more participate in the activity of innate immune regulation.

According to these findings, we conclude that VAT is more actively serving as energy storage but also serving as a primary coordinator of innate immune response compared with SAT. This conclusion is consistent with the study in drosophila innate immunity, which suggested that the fat body plays a significant role in energy storage and the innate immune response (Tzou et al., 2002).

5.6 ECM importance for subcutaneous adipose tissue

According to the different locations of visceral and subcutaneous adipose tissue, that subcutaneous fat is situated between the epithelial layer and muscle layer, we hypothesize that the expression of the genes related to tissue structure was different. The microarray result for extracellular matrix (ECM) may explain the difference.

We found out the close relationship between ECM and connected tissues exiting in SAT. This is proved by the upregulation of COL15A1 and COL7A1in SAT. Their gene products are implicated in the interaction between the intracellular matrix and the connected cells. fat. Collagen COL15A1 can adhere basement membranes to underlying connective tissue stroma, and COL7A1 is an anchoring fibril connecting the epithelia and the underlying stroma. This result is in accordance with the subcutaneous (dorsal fat) location in Atlantis salmon.

Besides, the upregulation of COL1A1 and COL2A1 was found and the latter was less expressed. The two genes serve to maintain the integrity of the extracellular matrix with the association of other collagen genes. For instance, type XI collagen also helps maintain the spacing and diameter of type II collagen fibrils and type XVI collagen assistant the fibril-forming of type I and II collagens. Some other genes from our microarray result have been shown to also participate in the construction and maintaining of filamentous

networks in the extracellular matrix of SAT, such as MATN2 and POSTNB gene. The expression of these genes involved in the integrity of ECM suggests the crucial role of ECM in SAT.

A study indicates that collagen 1 has the potential to promote cell adhesion and stimulate lipogenesis in the differentiation of adipose-derived stem cells (ASCs) into adipocytes (Zöller et al., 2019). A decreased concentration of the periostin, a component of the extracellular matrix, has been shown to be closely related to the metabolic dysfunction of adipose tissue in a mouse model, accompanying the decrease of lipid metabolism (Graja et al., 2018).

We concluded that the normal function and integrity of ECM in SAT are more important in maintaining metabolic function for SAT in comparison to VAT.

6 Conclusion

VAT has a 'hypertrophic' morphology with fewer but larger adipocytes, while SAT has a while adipose a 'hyperplastic' morphology with many adipocytes of a smaller size.

The smaller size of adipocytes in SAT contributes to providing high levels of energy supply. However, the bigger size of adipocytes in VAT is related to higher FFA mobilization and large lipids accumulation.

The higher levels of metabolic enzyme genes indicate the powerful ability of SAT as a direct energy supply site compared with VAT providing the FFAs that are transported to other organs for oxidation.

VAT has a higher insulin resistance compared with SAT being more insulin sensitive.

VAT is more actively serving as energy storage but also serving as a primary coordinator of the innate immune response compared with SAT.

In comparison to the ECM function in VAT, the normal function and integrity of ECM are more necessary to maintain the metabolic function of SAT.

This thesis shows the morphological differences between VAT and SAT regarding cell numbers, cell sizes, and size distribution. Besides, by comparing the gene transcriptome profile, this thesis provides information about the functional difference between VAT and SAT with respect to insulin resistance, immunity, energy and lipid metabolism, and extracellular matrix.

7 Reference list

Abumrad, N. A., el-Maghrabi, M. R., Amri, E. Z., Lopez, E. & Grimaldi, P. A. (1993). Cloning of a rat adipocyte membrane protein implicated in binding or transport of long-chain fatty acids that is induced during preadipocyte differentiation. Homology with human CD36. *Journal of Biological Chemistry*, 268 (24): 17665-17668. doi: https://doi.org/10.1016/S0021-9258(17)46753-6.

Adomas, A., Heller, G., Olson, Å., Osborne, J., Karlsson, M., Nahalkova, J., Van Zyl, L., Sederoff, R., Stenlid, J., Finlay, R., et al. (2008). Comparative analysis of transcript abundance in Pinus sylvestris after challenge with a saprotrophic, pathogenic or mutualistic fungus. *Tree Physiology*, 28 (6): 885-897. doi: 10.1093/treephys/28.6.885.

Albalat, A., Gutiérrez, J. & Navarro, I. (2005). Regulation of lipolysis in isolated adipocytes of rainbow trout (Oncorhynchus mykiss): the role of insulin and glucagon. *Comp Biochem Physiol A Mol Integr Physiol*, 142 (3): 347-54. doi: 10.1016/j.cbpa.2005.08.006.

Arner, P. (1995). Differences in lipolysis between human subcutaneous and omental adipose tissues. *Ann Med*, 27 (4): 435-8. doi: 10.3109/07853899709002451.

Ballard, F. J., Hanson, R. W. & Leveille, G. A. (1967). Phosphoenolpyruvate Carboxykinase and the Synthesis of Glyceride-Glycerol from Pyruvate in Adipose Tissue. *Journal of Biological Chemistry*, 242 (11): 2746-2750. doi: https://doi.org/10.1016/S0021-9258(18)99631-6.

Bernlohr, D. A., Jenkins, A. E. & Bennaars, A. A. (2002). Chapter 10 Adipose tissue and lipid metabolism. In vol. 36 *New Comprehensive Biochemistry*, pp. 263-289: Elsevier.

Bilinski, E. & Jonas, R. E. E. (1970). Effects of Coenzyme A and Carnitine on Fatty Acid Oxidation by Rainbow Trout Mitochondria. *Journal of the Fisheries Research Board of Canada*, 27 (5): 857-864. doi: 10.1139/f70-093.

Bjerkeng, B., Refstie, S., Fjalestad, K. T., Storebakken, T., Rødbotten, M. & Roem, A. J. (1997). Quality parameters of the flesh of Atlantic salmon (Salmo salar) as affected by dietary fat content and full-fat soybean meal as a partial substitute for fish meal in the diet. *Aquaculture*, 157 (3): 297-309. doi: https://doi.org/10.1016/S0044-8486(97)00162-2.

Björnheden, T., Jakubowicz, B., Levin, M., Odén, B., Edén, S., Sjöström, L. & Lönn, M. (2004). Computerized Determination of Adipocyte Size. *Obes Res*, 12 (1): 95-105. doi: 10.1038/oby.2004.13.

Björntorp, P. (1991). Metabolic implications of body fat distribution. *Diabetes Care*, 14 (12): 1132-43. doi: 10.2337/diacare.14.12.1132.

Boden, G. (1997). Role of Fatty Acids in the Pathogenesis of Insulin Resistance and NIDDM. *Diabetes*, 46 (1): 3-10. doi: 10.2337/diab.46.1.3.

Bou, M., Todorčević, M., Fontanillas, R., Capilla, E., Gutiérrez, J. & Navarro, I. (2014). Adipose tissue and liver metabolic responses to different levels of dietary carbohydrates in gilthead sea bream (Sparus aurata). *Comp Biochem Physiol A Mol Integr Physiol*, 175: 72-81. doi: 10.1016/j.cbpa.2014.05.014.

Bou, M., Montfort, J., Le Cam, A., Rallière, C., Lebret, V., Gabillard, J.-C., Weil, C., Gutiérrez, J., Rescan, P.-Y., Capilla, E., et al. (2017). Gene expression profile during proliferation and differentiation of rainbow trout adipocyte precursor cells. *BMC Genomics*, 18 (1): 347-347. doi: 10.1186/s12864-017-3728-0.

Bouloumié, A., Sengenès, C., Portolan, G., Galitzky, J. & Lafontan, M. (2001). Adipocyte produces matrix metalloproteinases 2 and 9: involvement in adipose differentiation. *Diabetes*, 50 (9): 2080-6. doi: 10.2337/diabetes.50.9.2080.

Bouraoui, L., Gutiérrez, J. & Navarro, I. (2008). Regulation of proliferation and differentiation of adipocyte precursor cells in rainbow trout (Oncorhynchus mykiss). *Journal of Endocrinology*, 198 (3): 459. doi: 10.1677/joe-08-0264.

Brown, D. A. (2001). Lipid droplets: Proteins floating on a pool of fat. *Curr Biol*, 11 (11): R446-R449. doi: 10.1016/S0960-9822(01)00257-3.

Campisi, J. & d'Adda di Fagagna, F. (2007). Cellular senescence: when bad things happen to good cells. *Nat Rev Mol Cell Biol*, 8 (9): 729-740. doi: 10.1038/nrm2233.

Cannon, B. & Nedergaard, J. (2004). Brown adipose tissue: function and physiological significance. *Physiol Rev*, 84 (1): 277-359. doi: 10.1152/physrev.00015.2003.

Caspar-Bauguil, S., Cousin, B., Galinier, A., Segafredo, C., Nibbelink, M., André, M., Casteilla, L. & Pénicaud, L. (2005). Adipose tissues as an ancestral immune organ: Site-specific change in obesity. *FEBS Lett*, 579 (17): 3487-3492. doi: 10.1016/j.febslet.2005.05.031.

Casteilla, L. & Dani, C. (2006). Adipose tissue-derived cells: from physiology to regenerative medicine. *Diabetes Metab*, 32 (5): 393-401. doi: 10.1016/S1262-3636(07)70297-5.

Charrière, G., Cousin, B., Arnaud, E., André, M., Bacou, F., Pénicaud, L. & Casteilla, L. (2003). Preadipocyte Conversion to Macrophage: EVIDENCE OF PLASTICITY*. *Journal of Biological Chemistry*, 278 (11): 9850-9855. doi: https://doi.org/10.1074/jbc.M210811200.

Chun, H.-S., Jeon, J., Pagire, H., Lee, J., Chung, H.-C., Park, M., So, J.-H., Ryu, J.-H., Kim, C.-H., Ahn, J., et al. (2013). Synthesis of LipidGreen2 and its application in lipid and fatty liver imaging. *Molecular bioSystems*, 9: 630-3. doi: 10.1039/c3mb70022d.

Cianflone, K., Zakarian, R., Couillard, C., Delplanque, B., Despres, J.-P. & Sniderman, A. (2004). Fasting acylation-stimulating protein is predictive of postprandial triglyceride clearance. *Journal of Lipid Research*, 45 (1): 124-131. doi: https://doi.org/10.1194/jlr.M300214-JLR200.

contributors, W. (2021a). *DAPI*: *Wikipedia, The Free Encyclopedia*. Available at: https://en.wikipedia.org/w/index.php?title=DAPI&oldid=1003936835 (accessed: 23 February).

contributors, W. (2021b). *DNA microarray*: *Wikipedia, The Free Encyclopedia*. Available at: https://en.wikipedia.org/w/index.php?title=DNA_microarray&oldid=998166731 (accessed: 4 January).

contributors, W. (2021c). *Interleukin 6*: *Wikipedia, The Free Encyclopedia.* Available at: https://en.wikipedia.org/w/index.php?title=Interleukin_6&oldid=1006301450 (accessed: 20 February).

contributors, W. (2021d). *Phalloidin*: *Wikipedia, The Free Encyclopedia.* Available at: https://en.wikipedia.org/w/index.php?title=Phalloidin&oldid=1004361517 (accessed: 23 February).

Cooper, J. A. (1987). Effects of cytochalasin and phalloidin on actin. *J Cell Biol*, 105 (4): 1473-8. doi: 10.1083/jcb.105.4.1473.

Crockett, E. L. & Sidell, B. D. (1993). Substrate selectivities differ for hepatic mitochondrial and peroxisomal beta-oxidation in an Antarctic fish, Notothenia gibberifrons. *The Biochemical journal*, 289 (Pt 2) (Pt 2): 427-433. doi: 10.1042/bj2890427.

da Silva Meirelles, L., Caplan, A. I. & Nardi, N. B. (2008). In Search of the In Vivo Identity of Mesenchymal Stem Cells. *STEM CELLS*, 26 (9): 2287-2299. doi: https://doi.org/10.1634/stemcells.2007-1122.

Davis, R., Aguirre, V., Uchida, T., Yenush, L. & White, M. F. (2000). The c-Jun NH₂-terminal Kinase Promotes Insulin Resistance during Association with Insulin Receptor Substrate-1 and Phosphorylation of Ser³⁰⁷*. *Journal of Biological Chemistry*, 275 (12): 9047-9054. doi: 10.1074/jbc.275.12.9047.

Deng, T., Lyon, Christopher J., Minze, Laurie J., Lin, J., Zou, J., Liu, Joey Z., Ren, Y., Yin, Z., Hamilton, Dale J., Reardon, Patrick R., et al. (2013). Class II Major Histocompatibility Complex Plays an Essential Role in Obesity-Induced Adipose Inflammation. *Cell Metabolism*, 17 (3): 411-422. doi: 10.1016/j.cmet.2013.02.009.

Díez, J. & Iglesias, P. (2003). The role of the novel adipocyte-derived hormone adiponectin in human disease. *European journal of endocrinology / European Federation of Endocrine Societies*, 148: 293-300. doi: 10.1530/eje.0.1480293.

Doherty, M. J., Ashton, B. A., Walsh, S., Beresford, J. N., Grant, M. E. & Canfield, A. E. (1998). Vascular Pericytes Express Osteogenic Potential In Vitro and In Vivo. *Journal of Bone and Mineral Research*, 13 (5): 828-838. doi: https://doi.org/10.1359/jbmr.1998.13.5.828.

Dos-Anjos, S. & Catalán, J. M. (2019). *Techniques and Processing Methods to Isolate Stem Cells and Stromal Vascular Fraction Cells*. Cham: Cham: Springer International Publishing. pp. 223-233.

Eaton, S. (2002). Control of mitochondrial β-oxidation flux. *Prog Lipid Res*, 41 (3): 197-239. doi: 10.1016/S0163-7827(01)00024-8.

Elmquist, J. K., Elias, C. F. & Saper, C. B. (1999). From lesions to leptin: hypothalamic control of food intake and body weight. *Neuron*, 22 (2): 221-32. doi: 10.1016/s0896-6273(00)81084-3.

Farrington-Rock, C., Crofts, N. J., Doherty, M. J., Ashton, B. A., Griffin-Jones, C. & Canfield, A. E. (2004). Chondrogenic and Adipogenic Potential of Microvascular Pericytes. *Circulation*, 110 (15): 2226-2232. doi: doi:10.1161/01.CIR.0000144457.55518.E5.

Fauconneau, B., Alami-Durante, H., Laroche, M., Marcel, J. & Vallot, D. (1995). Growth and meat quality relations in carp. *Aquaculture*, 129: 265-297. doi: 10.1016/0044-8486(94)00309-C.

Fauconneau, B., Andre, S., Chmaitilly, J., Le Bail, P.-Y., Krieg, F. & Kaushik, S. J. (1997). Control of skeletal muscle fibres and adipose cells size in the flesh of rainbow trout. *Journal of Fish Biology*, 50 (2): 296-314. doi: https://doi.org/10.1111/j.1095-8649.1997.tb01360.x.

Finke, J., Fritzen, R., Ternes, P., Lange, W. & Dölken, G. (1993). An improved strategy and a useful housekeeping gene for RNA analysis from formalin-fixed, paraffin-embedded tissues by PCR. *Biotechniques*, 14 (3): 448-53.

Frizzell, H., Fonseca, R., Christo, S. N., Evrard, M., Cruz-Gomez, S., Zanluqui, N. G., von Scheidt, B., Freestone, D., Park, S. L., McWilliam, H. E. G., et al. (2020). Organ-specific isoform selection of fatty acid–binding proteins in tissue-resident lymphocytes. *Science Immunology*, 5 (46): eaay9283. doi: 10.1126/sciimmunol.aay9283.

FrØyland, Lie & Berge. (2000). Mitochondrial and peroxisomal β-oxidation capacities in various tissues from Atlantic salmon Salmo salar. *Aquaculture nutrition*, 6 (2): 85-89. doi: 10.1046/j.1365-2095.2000.00130.x.

Fukumoto, S. & Fujimoto, T. (2002). Deformation of lipid droplets in fixed samples. *Histochem Cell Biol*, 118 (5): 423-428. doi: 10.1007/s00418-002-0462-7.

Gimble, J. M., Katz, A. J. & Bunnell, B. A. (2007). Adipose-Derived Stem Cells for Regenerative Medicine. *Circ Res*, 100 (9): 1249-1260. doi: 10.1161/01.RES.0000265074.83288.09.

Gökhan, S. H., Narinder, S. S. & Bruce, M. S. (1993). Adipose Expression of Tumor Necrosis Factor-α: Direct Role in Obesity-Linked Insulin Resistance. *Science*, 259 (5091): 87-91. doi: 10.1126/science.7678183.

Gough, P. & Myles, I. A. (2020). Tumor Necrosis Factor Receptors: Pleiotropic Signaling Complexes and Their Differential Effects. *Frontiers in immunology*, 11: 585880-585880. doi: 10.3389/fimmu.2020.585880.

Graja, A., Garcia-Carrizo, F., Jank, A. M., Gohlke, S., Ambrosi, T. H., Jonas, W., Ussar, S., Kern, M., Schürmann, A., Aleksandrova, K., et al. (2018). Loss of periostin occurs in aging adipose tissue of mice and its genetic ablation impairs adipose tissue lipid metabolism. *Aging Cell*, 17 (5): e12810. doi: 10.1111/acel.12810.

Gregoire, F. M., Smas, C. M. & Sul, H. S. (1998). Understanding adipocyte differentiation. *Physiol Rev*, 78 (3): 783-809. doi: 10.1152/physrev.1998.78.3.783.

Gregoire, F. M. (2001). Adipocyte differentiation: from fibroblast to endocrine cell. *Exp Biol Med (Maywood)*, 226 (11): 997-1002. doi: 10.1177/153537020122601106.

Hagve, T.-A., Christophersen, B. O. & Dannevig, B. H. (1986). Desaturation and chain elongation of essential fatty acids in isolated liver cells from rat and rainbow trout. *Lipids*, 21 (3): 202-205. doi: https://doi.org/10.1007/BF02534822.

Harms, M. J., Li, Q., Lee, S., Zhang, C., Kull, B., Hallen, S., Thorell, A., Alexandersson, I., Hagberg, C. E., Peng, X. R., et al. (2019). Mature Human White Adipocytes Cultured under Membranes Maintain Identity, Function, and Can Transdifferentiate into Brown-like Adipocytes. *Cell Rep*, 27 (1): 213-225.e5. doi: 10.1016/j.celrep.2019.03.026.

Heir, R. & Stellwagen, D. (2020). TNF-Mediated Homeostatic Synaptic Plasticity: From in vitro to in vivo Models. *Frontiers in cellular neuroscience*, 14: 565841-565841. doi: 10.3389/fncel.2020.565841.

Hemre, G. I., Mommsen, T. P. & Krogdahl, A. (2002). Carbohydrates in fish nutrition: effects on growth, glucose metabolism and hepatic enzymes. *Aquaculture nutrition*, 8 (3): 175-194. doi: 10.1046/j.1365-2095.2002.00200.x.

Hirosumi, J., Tuncman, G., Chang, L., Görgün, C. Z., Uysal, K. T., Maeda, K., Karin, M. & Hotamisligil, G. S. (2002). A central role for JNK in obesity and insulin resistance. *Nature*, 420 (6913): 333-336. doi: 10.1038/nature01137.

Hutley, L. J., Newell, F. M., Joyner, J. M., Suchting, S. J., Herington, A. C., Cameron, D. P. & Prins, J. B. (2003). Effects of rosiglitazone and linoleic acid on human preadipocyte differentiation. *Eur J Clin Invest*, 33 (7): 574-81. doi: 10.1046/j.1365-2362.2003.01178.x.

Jezierska, B., Hazel, J. R. & Gerking, S. D. (1982). Lipid mobilization during starvation in the rainbow trout, Salmo gairdneri Richardson, with attention to fatty acids. *Journal of Fish Biology*, 21 (6): 681-692. doi: https://doi.org/10.1111/j.1095-8649.1982.tb02872.x.

Kershaw, E. E. & Flier, J. S. (2004). Adipose tissue as an endocrine organ. *J Clin Endocrinol Metab*, 89 (6): 2548-56. doi: 10.1210/jc.2004-0395.

Kjær, M. A., Todorčević, M., Torstensen, B. E., Vegusdal, A. & Ruyter, B. (2008). Dietary n-3 HUFA Affects Mitochondrial Fatty Acid β-Oxidation Capacity and Susceptibility to Oxidative Stress in Atlantic Salmon. *Lipids*, 43 (9): 813-827. doi: https://doi.org/10.1007/s11745-008-3208-z.

Kleveland, E. J., Syvertsen, B. L., Ruyter, B., Vegusdal, A., Jørgensen, S. M. & Gjøen, T. (2006). Characterization of scavenger receptor class B, type I in Atlantic salmon (Salmo salar L.). *Lipids*, 41 (11): 1017-1027. doi: 10.1007/s11745-006-5052-3.

Lago, F., Dieguez, C., Gómez-Reino, J. & Gualillo, O. (2007). The emerging role of adipokines as mediators of inflammation and immune responses. *Cytokine Growth Factor Rev*, 18 (3): 313-325. doi: 10.1016/j.cytogfr.2007.04.007.

Lin, Y., Rajala, M. W., Berger, J. P., Moller, D. E., Barzilai, N. & Scherer, P. E. (2001). Hyperglycemia-induced production of acute phase reactants in adipose tissue. *J Biol Chem*, 276 (45): 42077-83. doi: 10.1074/jbc.M107101200.

Liu, Z. J., Zhuge, Y. & Velazquez, O. C. (2009). Trafficking and differentiation of mesenchymal stem cells. *J Cell Biochem*, 106 (6): 984-991. doi: 10.1002/jcb.22091.

Maassen, J. A., Romijn, J. A. & Heine, R. J. (2007). Fatty acid-induced mitochondrial uncoupling in adipocytes as a key protective factor against insulin resistance and beta cell dysfunction: a new concept in the pathogenesis of obesity-associated type 2 diabetes mellitus. *Diabetologia*, 50 (10): 2036-2041. doi: 10.1007/s00125-007-0776-z.

MacDougald, O. A. & Rosen, E. D. (2006). Adipocyte differentiation from the inside out. *Nat Rev Mol Cell Biol*, 7 (12): 885-896. doi: 10.1038/nrm2066.

Makowski, L., Boord, J. B., Maeda, K., Babaev, V. R., Uysal, K. T., Morgan, M. A., Parker, R. A., Suttles, J., Fazio, S., Hotamisligil, G. S., et al. (2001). Lack of macrophage fatty-acid–binding protein aP2 protects mice deficient in apolipoprotein E against atherosclerosis. *Nature Medicine*, 7 (6): 699-705. doi: 10.1038/89076.

Mao, H. & Universitetet for miljø- og biovitenskap Institutt for husdyr- og, a. (2012). *Optimizing methods for studies of adipose tissue function in Atlantic salmon : with specific focus on isolation and culture conditions of adipocytes and whole adipose tissue fixation for morphological studies : master thesis (60 credits)*. Ås: H. Mao.

Mizuno, H., Zuk, P. A., Zhu, M., Lorenz, P. H., Benhaim, P. & Hedrick, M. H. (2002). Myogenic Differentiation by Human Processed Lipoaspirate Cells. *Plastic and Reconstructive Surgery*, 109 (1): 199-209.

Morgan, I. J., McCarthy, I. D. & Metcalfe, N. B. (2002). The influence of life-history strategy on lipid metabolism in overwintering juvenile Atlantic salmon. *Journal of Fish Biology*, 60 (3): 674-686. doi: https://doi.org/10.1111/j.1095-8649.2002.tb01693.x.

Murphy, K. M., Weaver, C., Mowat, A., Berg, L., Chaplin, D., Janeway, C. A., Travers, P. & Walport, M. (2017). *Janeway's immunobiology*.

Nanton, D. A., Vegusdal, A., Rørå, A. M. B., Ruyter, B., Baeverfjord, G. & Torstensen, B. E. (2007). Muscle lipid storage pattern, composition, and adipocyte distribution in different parts of Atlantic salmon (Salmo salar) fed fish oil and vegetable oil. *Aquaculture*, 265 (1): 230-243. doi: https://doi.org/10.1016/j.aquaculture.2006.03.053.

Nath, D., Heemels, M.-T. & Anson, L. (2006). Obesity and diabetes. *Nature*, 444 (7121): 839-839. doi: 10.1038/444839a.

Nishimura, S., Manabe, I., Nagasaki, M., Eto, K., Yamashita, H., Ohsugi, M., Otsu, M., Hara, K., Ueki, K., Sugiura, S., et al. (2009). CD8+ effector T cells contribute to macrophage recruitment and adipose tissue inflammation in obesity. *Nature Medicine*, 15 (8): 914-920. doi: 10.1038/nm.1964.

Ntambi, J. M. & Young-Cheul, K. (2000). Adipocyte differentiation and gene expression. *J Nutr*, 130 (12): 3122S-3126S. doi: 10.1093/jn/130.12.3122S.

Otto, T. C. & Lane, M. D. (2005). Adipose Development: From Stem Cell to Adipocyte. *Crit Rev Biochem Mol Biol*, 40 (4): 229-242. doi: 10.1080/10409230591008189.

Pickup, J. C., Mattock, M. B., Chusney, G. D. & Burt, D. (1997). NIDDM as a disease of the innate immune system: association of acute-phase reactants and interleukin-6 with metabolic syndrome X. *Diabetologia*, 40 (11): 1286-92. doi: 10.1007/s001250050822.

Podos, S. D., Agarwal, A. & Huang, M. (2018). Chapter 12 - Factor D. In Barnum, S. & Schein, T. (eds) *The Complement FactsBook (Second Edition)*, pp. 117-126: Academic Press.

Potter, B. J., Stump, D., Schwieterman, W., Sorrentino, D., Jacobs, L. N., Kiang, C. L., Rand, J. H. & Berk, P. D. (1987). Isolation and partial characterization of plasma membrane fatty acid binding proteins from myocardium and adipose tissue and their relationship to analogous proteins in liver and gut. *Biochem Biophys Res Commun*, 148 (3): 1370-1376. doi: 10.1016/S0006-291X(87)80283-8.

Rajala, M. W. & Scherer, P. E. (2003). Minireview: The Adipocyte—At the Crossroads of Energy Homeostasis, Inflammation, and Atherosclerosis. *Endocrinology*, 144 (9): 3765-3773. doi: 10.1210/en.2003-0580.

Ramírez-Zacarías, J. L., Castro-Muñozledo, F. & Kuri-Harcuch, W. (1992). Quantitation of adipose conversion and triglycerides by staining intracytoplasmic lipids with oil red O. *Histochemistry*, 97 (6): 493-497. doi: 10.1007/BF00316069.

Rangwala, S. & Lazar, M. (2000). Transcriptional control of adipogenesis. *Annual review of nutrition*, 20: 535-59. doi: 10.1146/annurev.nutr.20.1.535.

Refstie, S., Storebakken, T., Baeverfjord, G. & Roem, A. J. (2001). Long-term protein and lipid growth of Atlantic salmon (Salmo salar) fed diets with partial replacement of fish meal by soy protein products at medium or high lipid level. *Aquaculture*, 193 (1): 91-106. doi: https://doi.org/10.1016/S0044-8486(00)00473-7.

Rooijakkers, S. H. M., Wu, J., Ruyken, M., van Domselaar, R., Planken, K. L., Tzekou, A., Ricklin, D., Lambris, J. D., Janssen, B. J. C., van Strijp, J. A. G., et al. (2009). Structural and functional implications of the alternative complement pathway C3 convertase stabilized by a staphylococcal inhibitor. *Nature immunology*, 10 (7): 721-727. doi: 10.1038/ni.1756.

Rørå, A., Kvåle, A., Mørkøre, T., Rørvik, K.-A., Steien, S. H. & Thomassen, S. (1998). Process yield, colour and sensory quality of smoked Atlantic salmon (Salmo salar) in relation to raw material characteristics. *Food Research International*, 31: 601-609. doi: 10.1016/S0963-9969(99)00034-4.

Rosen, E. D., Walkey, C. J., Puigserver, P. & Spiegelman, B. M. (2000). Transcriptional regulation of adipogenesis. *Genes Dev*, 14 (11): 1293-1307.

Rowe, D. K., Thorpe, J. E. & Shanks, A. M. (1991). Role of Fat Stores in the Maturation of Male Atlantic Salmon (Salmo salar) Parr. *Canadian Journal of Fisheries and Aquatic Sciences*, 48 (3): 405-413. doi: 10.1139/f91-052.

Salmerón, C., Riera-Heredia, N., Gutiérrez, J., Navarro, I. & Capilla, E. (2016). Adipogenic Gene Expression in Gilthead Sea Bream Mesenchymal Stem Cells from Different Origin. *Front Endocrinol (Lausanne)*, 7: 113-113. doi: 10.3389/fendo.2016.00113.

Schaffer, J. E. & Lodish, H. F. (1994). Expression cloning and characterization of a novel adipocyte long chain fatty acid transport protein. *Cell*, 79 (3): 427-436. doi: https://doi.org/10.1016/0092-8674(94)90252-6.

Schulz, H. (2002). Chapter 5 Oxidation of fatty acids in eukaryotes. In vol. 36 *New Comprehensive Biochemistry*, pp. 127-150: Elsevier.

Sheridan, M. A. (1988). Lipid dynamics in fish: aspects of absorption, transportation, deposition and mobilization. *Comparative Biochemistry and Physiology Part B: Comparative Biochemistry*, 90 (4): 679-690. doi: https://doi.org/10.1016/0305-0491(88)90322-7.

Sims, J., March, C., Cosman, D., Widmer, M., MacDonald, H., McMahan, C., Grubin, C., Wignall, J., Jackson, J., Call, S., et al. (1988). cDNA expression cloning of the IL-1 receptor, a member of the immunoglobulin superfamily. *Science*, 241 (4865): 585-589. doi: 10.1126/science.2969618.

Skalli, O., Pelte, M. F., Peclet, M. C., Gabbiani, G., Gugliotta, P., Bussolati, G., Ravazzola, M. & Orci, L. (1989). Alpha-smooth muscle actin, a differentiation marker of smooth muscle cells, is present in microfilamentous bundles of pericytes. *Journal of Histochemistry & Cytochemistry*, 37 (3): 315-321. doi: 10.1177/37.3.2918221.

Škugor, A. (2009). *Transcriptome responses in adipose-derived stromo vascular fraction of Atlantic salmon (Salmo salar) induced by lipopolysaccharide*. Ås: A. Škugor.

Slawik, M. & Vidal-Puig, A. J. (2007). Adipose tissue expandability and the metabolic syndrome. *Genes & nutrition*, 2 (1): 41-45. doi: 10.1007/s12263-007-0014-9.

Tandon, P., Wafer, R. & Minchin, J. E. N. (2018). Adipose morphology and metabolic disease. *J Exp Biol*, 221 (Pt Suppl 1). doi: 10.1242/jeb.164970.

Tauchi-Sato, K., Ozeki, S., Houjou, T., Taguchi, R. & Fujimoto, T. (2002). The Surface of Lipid Droplets Is a Phospholipid Monolayer with a Unique Fatty Acid Composition*. *Journal of Biological Chemistry*, 277 (46): 44507-44512. doi: https://doi.org/10.1074/jbc.M207712200.

Todorcevic, M., Ruyter, B. & Vegusdal, A. (2009). *Development and functions of adipose tissue in Atlantic salmon*. Fettvevets utvikling og funksjoner i atlantisk laks: Norwegian University of Life Sciences, Ås.

Todorčević, M., Vegusdal, A., Gjøen, T., Sundvold, H., Torstensen, B. E., Kjær, M. A. & Ruyter, B. (2008). Changes in fatty acids metabolism during differentiation of Atlantic salmon preadipocytes; Effects of n-3 and n-9 fatty acids. *Biochimica et Biophysica Acta (BBA) - Molecular and Cell Biology of Lipids*, 1781 (6): 326-335. doi: https://doi.org/10.1016/j.bbalip.2008.04.014.

Todorčević, M., Škugor, S., Krasnov, A. & Ruyter, B. (2010). Gene expression profiles in Atlantic salmon adipose-derived stromo-vascular fraction during differentiation into adipocytes. *BMC Genomics*, 11 (1): 39. doi: 10.1186/1471-2164-11-39.

Tontonoz, P., Nagy, L., Alvarez, J. G. A., Thomazy, V. A. & Evans, R. M. (1998). PPARγ Promotes Monocyte/Macrophage Differentiation and Uptake of Oxidized LDL. *Cell (Cambridge)*, 93 (2): 241-252. doi: 10.1016/S0092-8674(00)81575-5.

Torstensen, B. E., Nanton, D. A., Olsvik, P. A., Sundvold, H. & Stubhaug, I. (2009). Gene expression of fatty acid-binding proteins, fatty acid transport proteins (cd36 and FATP) and β-oxidation-related genes in Atlantic salmon (Salmo salar L.) fed fish oil or vegetable oil. *Aquaculture nutrition*, 15 (4): 440-451. doi: 10.1111/j.1365-2095.2008.00609.x.

Traktuev, D. O., Merfeld-Clauss, S., Li, J., Kolonin, M., Arap, W., Pasqualini, R., Johnstone, B. H. & March, K. L. (2008). A Population of Multipotent CD34-Positive Adipose Stromal Cells Share Pericyte and Mesenchymal Surface Markers, Reside in a Periendothelial Location, and Stabilize Endothelial Networks. *Circ Res*, 102 (1): 77-85. doi: 10.1161/CIRCRESAHA.107.159475.

Trigatti, B. L., Anderson, R. G. W. & Gerber, G. E. (1999). Identification of Caveolin-1 as a Fatty Acid Binding Protein. *Biochem Biophys Res Commun*, 255 (1): 34-39. doi: 10.1006/bbrc.1998.0123.

Tzou, P., De Gregorio, E. & Lemaitre, B. (2002). How Drosophila combats microbial infection: a model to study innate immunity and host-pathogen interactions. *Curr Opin Microbiol*, 5 (1): 102-10. doi: 10.1016/s1369-5274(02)00294-1.

Ugye, J. (2010). Formaldehyde as a Contrast Enhancer in Gram's Staining Analysis. Journal of Applied Sciences Research, 6 (3): 269 – 271. 6(3): 269-271.

van Greevenbroek, M. M., Ghosh, S., van der Kallen, C. J., Brouwers, M. C., Schalkwijk, C. G. & Stehouwer, C. D. (2012). Up-regulation of the complement system in subcutaneous adipocytes from nonobese, hypertriglyceridemic subjects is associated with adipocyte insulin resistance. *J Clin Endocrinol Metab*, 97 (12): 4742-52. doi: 10.1210/jc.2012-2539.

Van Harmelen, V., Reynisdottir, S., Cianflone, K., Degerman, E., Hoffstedt, J., Nilsell, K., Sniderman, A. & Arner, P. (1999). Mechanisms involved in the regulation of free fatty acid release from isolated human fat cells by acylation-stimulating protein and insulin. *J Biol Chem*, 274 (26): 18243-51. doi: 10.1074/jbc.274.26.18243.

Vegusdal, A., Sundvold, H., Gjøen, T. & Ruyter, B. (2003). An in vitro method for studying the proliferation and differentiation of Atlantic salmon preadipocytes. *Lipids*, 38 (3): 289-96. doi: 10.1007/s11745-003-1063-3.

Wajchenberg, B. L. (2000). Subcutaneous and visceral adipose tissue: their relation to the metabolic syndrome. *Endocr Rev*, 21 (6): 697-738. doi: 10.1210/edrv.21.6.0415.

Wei, T., Daniel, Z., Jae Myoung, S., Darko, B., Michael, K., Robert, E. H., Michelle, D. T. & Jonathan, M. G. (2008). White Fat Progenitor Cells Reside in the Adipose Vasculature. *Science*, 322 (5901): 583-586. doi: 10.1126/science.1156232.

Weil, C., Lefèvre, F. & Bugeon, J. (2013). Characteristics and metabolism of different adipose tissues in fish. *Reviews in Fish Biology and Fisheries*, 23 (2): 157-173. doi: 10.1007/s11160-012-9288-0.

Yang, Y. K., Chen, M., Clements, R. H., Abrams, G. A., Aprahamian, C. J. & Harmon, C. M. (2008). Human mesenteric adipose tissue plays unique role versus subcutaneous and omental fat in obesity related diabetes. *Cell Physiol Biochem*, 22 (5-6): 531-8. doi: 10.1159/000185527.

Ytteborg, E., Vegusdal, A., Witten, P. E., Berge, G. M., Takle, H., Østbye, T.-K. & Ruyter, B. (2010). Atlantic salmon (Salmo salar) muscle precursor cells differentiate into osteoblasts in vitro: Polyunsaturated fatty acids and hyperthermia influence gene expression and differentiation. *Biochimica et biophysica acta. Molecular and cell biology of lipids*, 1801 (2): 127-137. doi: 10.1016/j.bbalip.2009.10.001.

Ytteborg, E., Todorcevic, M., Krasnov, A., Takle, H., Kristiansen, I. Ø. & Ruyter, B. (2015). Precursor cells from Atlantic salmon (Salmo salar) visceral fat holds the plasticity to differentiate into the osteogenic lineage. *Biology Open*, 4 (7): 783-791. doi: 10.1242/bio.201411338.

Zannettino, A. C. W., Paton, S., Arthur, A., Khor, F., Itescu, S., Gimble, J. M. & Gronthos, S. (2008). Multipotential human adipose-derived stromal stem cells exhibit a perivascular phenotype in vitro and in vivo. *J Cell Physiol*, 214 (2): 413-421. doi: 10.1002/jcp.21210.

Zemel, M. B., Shi, H., Greer, B., Dirienzo, D. & Zemel, P. C. (2000). Regulation of adiposity by dietary calcium. *Faseb j*, 14 (9): 1132-8.

Zemel, M. B. (2003). Mechanisms of dairy modulation of adiposity. *J Nutr*, 133 (1): 252s-256s. doi: 10.1093/jn/133.1.252S.

Zhang, Y., Proenca, R., Maffei, M., Barone, M., Leopold, L. & Friedman, J. M. (1994). Positional cloning of the mouse obese gene and its human homologue. *Nature*, 372 (6505): 425-32. doi: 10.1038/372425a0.

Zhol, S., Ackman, R. G. & Morrison, C. (1995). Storage of lipids in the myosepta of Atlantic salmon (Salmo salar). *Fish Physiology and Biochemistry*, 14 (2): 171-178. doi: 10.1007/BF00002460.

Zhou, S., Ackman, R. G. & Morrison, C. (1996). Adipocytes and lipid distribution in the muscle tissue of Atlantic salmon (Salmo salar). *Canadian Journal of Fisheries and Aquatic Sciences*, 53 (2): 326-332. doi: 10.1139/f95-197.

Zimmerlin, L., Donnenberg, V. S., Pfeifer, M. E., Meyer, E. M., Péault, B., Rubin, J. P. & Donnenberg, A. D. (2010). Stromal vascular progenitors in adult human adipose tissue. *Cytometry A*, 77A (1): 22-30. doi: 10.1002/cyto.a.20813.

Zöller, N., Schreiner, S., Petry, L., Hoffmann, S., Steinhorst, K., Kleemann, J., Jäger, M., Kaufmann, R., Meissner, M. & Kippenberger, S. (2019). Collagen I Promotes Adipocytogenesis in Adipose-Derived Stem Cells In Vitro. *Cells*, 8 (4): 302. doi: 10.3390/cells8040302.